THE DIAGNOSTICS OF PLASMAS*

JOHN A. THORNTON,† RICHARD C. WARDER JR.,† and
ALI BULENT CAMBEL

Gas Dynamics Laboratory, Northwestern University,
Evanston, Illinois, U.S.A.

In energy conversion processes, both natural and man-made plasmas may be used to advantage. However, regardless of origin, it is necessary to know the properties of plasmas before reliable energy conversion devices can be designed and constructed. It is the purpose of this paper to highlight the theoretical considerations underlying plasma diagnostic techniques used in the Gas Dynamics Laboratory in conjunction with a variety of plasma generation facilities.

Dans les processus de conversion de l'énergie on peut utiliser aussi bien les plasmas naturels que les plasmas artificiels. Cependant quelle que soit l'origine de ces plasmas il convient de connaître leurs propriétés avant que des systèmes de conversion à fonctionnement sûr puissent être conçus et réalisés. Le présent mémoire analyse les principales considérations théoriques sur lesquelles sont basées les techniques de diagnostic des plasmas, ainsi que les générateurs de plasma utilisés.

INTRODUCTION

To design plasma facilities and devices rationally, it is necessary to know the various plasma properties. Although these can be calculated from theoretical considerations, it is proper to seek experimental verification. Such experimental measurements are doubly necessary because there is no consensus as to which among contradictory theories and hypotheses is applicable to one type of plasma or another.

The high temperatures encountered in plasma facilities rule out most of the conventional measurement techniques. The reasons for this are multifold. First, a plasma encountered in most engineering problems consists of a mixture of neutral atoms and/or molecules, electrons, negative and possibly charged ions. Thus it is necessary to know the chemical composition and the respective concentration of the constituents. Second, in many practical cases, the plasma experiences physico-chemical reactions making it necessary to be careful with measurements which might rely on equilibrium

* Summary version of invited paper prepared for the Sixth AGARD Combustion and Propulsion Colloquium, "Energy Sources and Energy Conversion", Cannes, France (March 16–March 20, 1964).

† Present Address: Space Sciences Laboratory, Litton Systems, Inc., Beverly Hills, California.

considerations. Third, the plasma diagnostician will have to realize that the medium is electrically conducting and thus many measurement techniques perfected for high-speed, high-temperature neutral gases must be modified. Fourth, the very high-temperatures encountered in plasmas make difficult the choice of materials which have to withstand high thermal energy fluxes. Fifth, the very high temperatures associated with plasmas suggest that radiation effects cannot be neglected without due deliberation. Sixth,

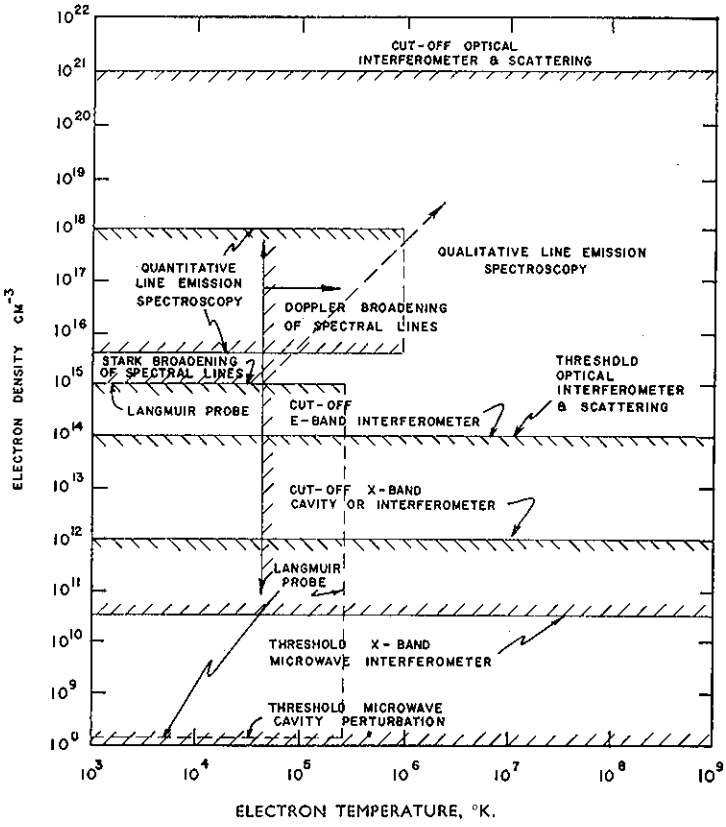

Fig. 1. Regions of application for various diagnostic techniques.

most engineering devices involve high-velocity turbulent flow, which inherently complicates the measurements. Thus, one must be careful in differentiating between the true properties of the plasma gas and the apparent properties of the plasma stream. Further, any probes introduced into the flow will disturb and alter the flow pattern. Seventh, in plasma probing, a non-neutral plasma sheath forms on solid boundaries and hence, the data must be interpreted with considerable care. Eighth, when a magnetic field is applied to the plasma, the properties may assume directional characteristics.

As may be inferred from the aforementioned it is difficult, if not impossible, to classify the numerous diagnostic techniques. However, it is helpful to arrange the available measurements on a diagnostic map as shown in Fig. 1 wherein the different techniques are arranged according to their applicable regions of electron density and temperature. It should be emphasized that this map is not categoric and should be treated as a preliminary guide only. Thus, it must be realized that the regions of applicability will vary with the specific circumstances under which plasmas may be encountered. Furthermore, the usefulness of the different instruments are being extended by researchers in the field.

Certain limitations of this paper should be pointed out. Thus, the measurements which are described were conducted with argon, nitrogen, air, and hydrocarbon plasmas generated in combustion tunnels, arc jetc, arc columns and electromagnetic shock tubes. The gas pressures were atmospheric or subatmospheric. The range of electron temperatures was 3000° to 20,000° K and the electron densities were as high as 10^{18} cm^{-3}. Nevertheless, it should be appreciated that the techniques discussed are not limited to the aforementioned circumstances, but can be adapted to other conditions provided the theoretical circumstances warrant this. Accordingly, the intricacies of instrument construction are sacrificed in this paper in favor of theoretical considerations and the interpretation of the data. Although a variety of techniques are described, not all research in plasma diagnostics could be mentioned because of space limitations. Indeed the major emphasis is placed on a portion of the studies being conducted in the Gas Dynamics Laboratory. At the time of preparing this present paper for the printer a general survey of plasma diagnostics appeared and is cited as (Ref. 1).

DESCRIPTION OF THE PLASMA

There is no "best" sequence of measurements which must be followed in plasma diagnostics. However, it is helpful to answer certain questions at an early stage of magnetogasdynamic research. These are: (a) is the plasma optically transparent; (b) is it homogeneous; (c) what is the flow configuration; and (d) is the plasma in equilibrium? It should be noted that these characteristics are both macroscopic and microscopic in nature.

Optical transparency: A plasma is said to be optically thin when it does not absorb appreciably the radiation which it emits. The extent of the plasma transparency is an important factor in any measurement relying on radiative phenomena and in attempting to determine the configuration of the flow.

The optical thickness of plasma streams may be determined either analytically or by experiment. Thus, Olsen (Ref. 2) has confirmed the transparency of atmospheric argon plasmas by calculating the absorption coefficients for the atomic lines. This can be accomplished by determining experimentally the temperature profile and then obtaining the absorption coefficients from iterative corrections to the intensity profiles.

We have used (Ref. 3) a very simple experiment. A spectroscope is placed at one side of the plasma stream and a schlieren-type parabolic mirror on

the other. First, the mirror is covered so that the radiation intensity recorded is that which is due to the plasma radiation viewed by the spectroscope. Next the mirror is uncovered and the image of the luminous jet is focused by the mirror with a 1:1 magnification upon itself. This reflected image passing through the plasma arc falls upon the spectroscope. We have found that with transparent plasmas there is an increase of about 95 per cent in the intensity as may be seen in Fig. 2. This is an adequate test for optical transparency because the mirror itself is not a perfect reflector.

At very low pressures when the optical thickness is too little, even the most sensitive of conventional optical instrumentation such as schlieren and

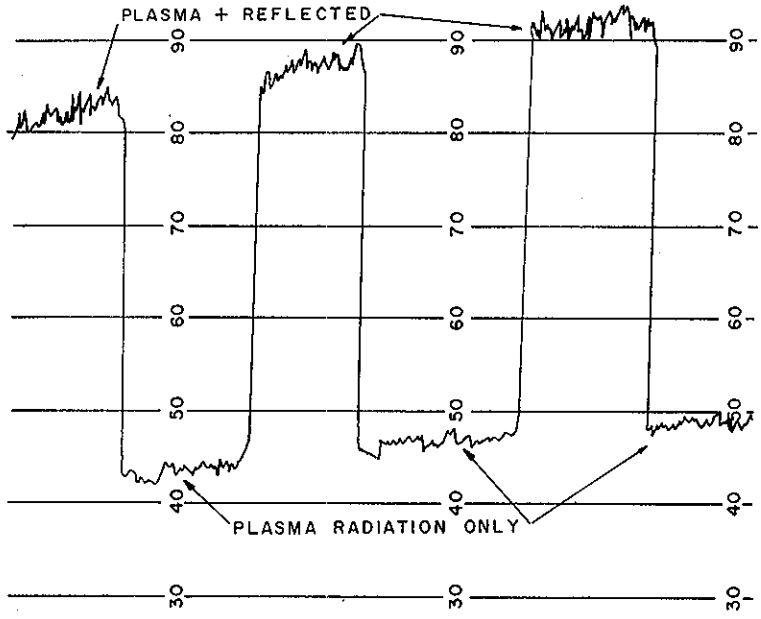

Fig. 2. Transparency test.

interferometry may be inadequate. However, because plasmas are luminescent, crude flow visualization is possible by photography. The luminescence will depend on the gas used but may be accentuated by adding small amounts of tracer gases such as oxygen and nitric oxide. Of course, the tracer gas should be introduced in sufficiently small quantities so that the electrical properties of the gas will not be modified significantly and so that the fluid mechanics will not be distorted.

Plasma homogeneity

Many diagnostic techniques, such as microwave measurements, involve the assumption that the plasma being diagnosed can be represented by a slab. Thus, one may wish to know the extent of boundary effects and gradients at the interface. A gross indication of the plasma homogeneity may be

had by measuring the light intensity variation across the plasma. This can be accomplished (Ref. 4) with a simple apparatus consisting of a photocell or photomultiplier tube in a black box with an appropriate collimation system. This detector is used in traversing the plasma in the direction desired, and its output is fed to an oscilloscope. Ideally, for a plasma with discrete interfaces the light intensity variation should behave like a step function. Although actually this will not be the case, one can assume that the plasma configuration satisfies the theoretical assumptions regarding discrete interfaces and homogeneity if the measured light intensity variation manifests a rather sharp and uniform increase.

In the absence of sophisticated photographic apparatus such as a Kerr Cell a bank of such photomultiplier tubes, closely spaced, may be used (Ref. 5) in determining the shape of the luminous front in electromagnetic shock tubes.

Flow configuration

The configuration of plasmas can be observed in a global way by means of photography and in a more intimate sense by probing.

Because of the extreme radiation intensity of the plasma and the variation of the parameters which influence the intensity, the experimenter is faced in plasma photography (Refs. 6 and 7) with the time-consuming task of determining more or less by trial and error which films, filters and exposure indices to use.

In general, in arc jet facilities variations of the gas flow rate, power input and test section conditions influence the gross radiation intensity less than they do the arc fluid mechanics. However, the electrode gap has a very marked effect on the intensity of the arc because of its effect on the voltage drop across the electrodes.

Because plasma tunnels are frequently operated over a wide range of power inputs, it is helpful to obtain a relation between the arc intensity and the power input. This is done best by keeping the electrode spacing constant so that the voltage drop across the electrodes does not vary appreciably. An empirical equation of the following form may then be written

$$I = C_1 P^{C_2} \tag{1}$$

where I is the intensity of illumination in ft-c, P is the power input to the arc in kw, C_1 and C_2 are experimental constants for any particular arc jet facility.

To determine the exposure, graphs of basic f-stops vs arc power are made. These should be corrected for the f/stops for films of different ASA ratings and for different arc-to-lens distances.

It is evident that the experimenter must adapt the photography to his particular needs. However, we shall mention some thumb rules for the experimenter's convenience. For argon plasma arc jets, Kodak-Panatomic-X film gives good results with filters having an optical density of about 4 for f/5·6 and an exposure of 1/250 sec.

Color photography is most revealing and may be undertaken by using the exposure index determined for black-and-white photography as a guide.

(Trial and error in color photography is not recommended because of the expense and the long development period.) Depending on the gas used, its plasma will have a different color or hue. The general rule in the photography of self-illuminated objects is to use a film having the same spectral response. We have found that with supersonic argon plasma flows Kodachrome Type B film with f/16 at 1/30 sec. gives excellent results.

Care must be exercised in determining the proper exposure index because a clear photograph is not necessarily a true picture of the arc. This is due to the fact that there are severe temperature gradients which affect the radiation. Thus, the boundaries of the plasma regime are diffuse and should be checked with other techniques.

High-speed motion pictures of plasma streams are revealing to study unstable arc conditions, particularly during the initiation and stabilization of arcs. The main difficulty which may be encountered is that during the formation of the arc column, its intensity varies radically whereas the exposure latitude of most films is relatively narrow. Therefore, it may be expedient to edit and splice films taken at different exposures.

In connection with flow visualization it should be mentioned that both the Toepler-schlieren system (Ref. 8) and the Mach-Zehnder interferometer are very useful. The latter is also a potent instrument in determining (Ref. 9) the electron density of plasmas. Due to space limitations we will not discuss these here further.

The measurement of pressure

In general pressure measurements in plasmas are quite similar to the approach followed in classical gasdynamics.

The static pressure in the streaming section of continuous flow plasma facilities may be determined with reasonable reliability by means of a static pressure probe. However, the low density and high enthalpy encountered in hypersonic plasma arcs introduce errors which must be evaluated carefully.

The impact pressure may be determined in general by the use of water-cooled impact tubes which we use with reasonable satisfaction. Of course, in the case of partially ionized gases which one encounters in plasma arc jets, errors are introduced because the thermophysical properties are not well known and because recombination reactions may be expected to occur. However, it has been shown by Grey, Jacobs and Sherman (Ref. 10) that the impact pressure measurements are substantially unaffected by ion recombination in the detached shock ahead of the probe.

In electromagnetic shock tube studies the state of the gas behind the shock can be estimated readily if the initial pressure and the density of the gas and the shock velocity are known. The initial pressure should be measured, therefore, with accuracy and this can be done with an ionization pressure gage or a McLeod gage. In our work we use commerically available Alphatron gages. These give data within an accuracy of about 4 per cent at pressures above 10 microns of mercury.

Direct measurements of pressure after the shock tube has been fired are inherently difficult because, particularly at high velocities, the response of gages is too slow. Nevertheless, the pressure or its variation may be obtained from the shock velocities, and a variety of instruments have been developed (Ref. 11).

Spectroscopic determination of velocity distribution

We shall not discuss here in detail the measurements leading to plasma flow velocity and shock velocity because they are treated extensively in the literature (Refs. 1 and 12). However, we present here the spectroscopic determination (Ref. 13) of the velocity distribution in steady-flow arc jets.

In the absences of external fields, the energy equation in cylindrical coordinates may be written as follows:

$$\rho c_p V_z \frac{\partial T}{\partial z} = \vec{J}\cdot\vec{E} + \frac{\partial K(T)}{\partial T}\left[\left(\frac{\partial T}{\partial r}\right)^2 + \left(\frac{\partial T}{\partial z}\right)^2\right] + K(T)\left[\frac{\partial^2 T}{\partial r^2} + \frac{1}{r}\frac{\partial T}{\partial r} + \frac{\partial^2 T}{\partial z^2}\right] \qquad (2)$$

The assumptions inherent in this equation are (a) the flow is steady and fluctuations in the arc power supply are negligible; (b) the velocity in the luminous arc is in the axial z-direction and radial and azimuthal components are negligible. In typical laboratory studies with argon plasmas we have found that the radial velocity is about 1% or less of the axial velocity; (c) changes of the kinetic energy in the axial direction are small in comparison with changes of the enthalpy. Computations show that this assumption is valid within an error of less than 1%; (d) energy dissipation due to viscous effects are small compared to heat transfer by convection and conduction; (e) radiative heat losses are small compared to heat losses by convection and conduction. Measurements (Ref. 14) indicate that this later assumption is more pertinent to nitrogen plasmas than to argon plasmas.

The axial velocity distribution is then calculated from the energy equation because the temperature distribution is known from the spectroscopic measurements. In turn values of c_p and ρ may be found from the calculations which we have presented (Refs. 15, 16, 17) elsewhere. Values of the thermal conductivity have been calculated by Bosnjakovic and Springe (Ref. 18) and by Cann (Ref. 19). Spectroscopic measurements of the thermal conductivity have been made by our colleague Knopp (Ref. 20) and these indicate that Cann's calculations are very reasonable.

PHYSICAL-CHEMICAL CHARACTERISTICS

One of the most important objectives of the experimentalist is to determine the state, and if applicable the thermodynamic state, of the system he is working with. When dealing with plasmas one must consider real gas effects such as the excitation of the internal states of atoms and ions and molecules.

dissociation, ionization, radiation, interparticle forces, and quantum mechanical effects. Even though the interrelationships among these processes are complex, when a single species system is in complete equilibrium* the thermodynamic state can be completely specified, in principle at least, by two independent state variables.† Although this apparent simplicity of the thermodynamic formalism is of considerable importance in purely analytical studies, we have found a slightly redundant multicomponent specification of the thermodynamic state more useful in experimental studies (Ref. 21) and in analytical studies which are to be used in conjuction with experimental work (Ref. 15). This is because many of the most useful plasma diagnostic tools provide information on component properties rather than the bulk properties such as total pressure and density. Furthermore, in laboratory plasmas one frequently encounters situations in which the various degrees of freedom within the plasma are in equilibrium with themselves but not with each other. These situations of incomplete equilibrium occur because of the differing rates for the various collisional and radiative energy transfer processes which control the populations of the different degrees of freedom. That is, when the rates of energy transfer are such that the particles can freely exchange energy between the energy levels within a given degree of freedom and thus rapidly come into an equilibrium (Boltzmann) distribution for those energy levels, but are energetically isolated with respect to the different degrees of freedom, it is useful to treat each degree of freedom as an isolated thermodynamic system and therefore to associate with each an appropriate temperature. The mass difference between the electrons and the atoms and ions in a plasma results in such an isolation.

In the multicomponent model one specifies the temperature and number densities associated with each degree of freedom. Consider a partially ionized monatomic plasma. Let us assume that it is a quasi-equilibrium plasma; that is, we assume that each degree of freedom can be treated as an isolated equilibrium thermodynamic subsystem. The plasma will be composed of electrons, atoms and ions of the test gas, and atoms and ions from impurities. Impurities will always be present to some extent in laboratory generated plasmas; for the purposes of this discussion we shall assume only one species. The appropriate subsystems are summarized in Table 1 along with the state variables required for their specification. Useful methods of plasma diagnostics are summarized‡ in Table 2 in terms of the degrees of freedom about which they provide information. The bound electronic states within the atoms and ions constitute a particular case. The amount of energy stored in these states is usually small compared to the translational energies of the particles. Furthermore, unlike the degree of ionization, they

* Strictly speaking, complete equilibrium requires that the plasma be in equilibrium with the walls of its container. It is obvious that this criterion is seldom if ever satisfied in the laboratory.

† Thermodynamic effects due to electromagnetic fields will be neglected throughout this discussion.

‡ For a more complete list see Ref. 12.

Table 1

State	*State variable*	
Free States:		
Electron translational states	T_e	N_e
Test gas atom translational states	T_a	N_a
Test gas ion translational states	T_i	N_i
Impurity atom translational states	$\overline{T}_a$	$\overline{T}_a$
Impurity ion translational states	$\overline{T}_i$	$\overline{T}_i$
Bound Electronic States:		
Test gas atom internal bound states	(T_e)	$\{N_{an}\}$
Test gas ion internal bound states	(T_e)	$\{N_{in}\}$
Impurity atom internal bound states	(T_e)	$\{\overline{N}_{an}\}$
Impurity ion internal bound states	(T_e)	$\{\overline{N}_{in}\}$

do not affect gross plasma properties* such as the electrical conductivity. However, they are very important in the use of line emission spectroscopy for quantitative plasma measurements and accordingly have been included

Table 2

Electron translational degree of freedom
- N_e—Microwave methods,
  - Conductivity probes
  - Optical interferometry
  - Continuum radiation in optical region
  - Particle collectors
  - Electron or ion beam scattering
- T_e—Langmuir probes
  - Microwave radiation

Atom translational degrees of freedom
- N_a—Shielded ionization gauge
  - Ion or neutral atom beam scattering
  - Charge exchange detectors
- T_a—Doppler broadening of atomic spectral lines

Ion translational degrees of freedom
- N_i—Langmuir probes
  - Stark broadening of spectral lines
  - Electron, ion, neutral atom or neutron beam probes
- T_i—Doppler broadening of ion spectral lines

Bound electronic states
- N_n—Spectral line emission and absorption
- (T_e)—Spectral line emission (if bound states are in equilibrium with the free electrons)

in Tables 1 and 2. Unless very strong fields are present and the plasma density is low, $T_a = T_i = T_g$ where we define T_g as the gas or heavy

* An obvious exception to this statement would of course be the gaseous laser, in which the performance depends on the relative bound state populations.

particle temperature. Thus, for the quasi-equilibrium plasma being considered, the results of the plasma diagnostician's efforts will ideally be a specification of the plasma thermodynamic state in terms of the following set of variables,

$$[T_e,\ T_g,\ N_e\ N_a,\ \bar{N}_a,\ \bar{N}_i] \tag{3}$$

which clearly indicates departures from thermal equilibrium and impurity levels.

Each of the experimental methods listed in Table 2 is applicable only within a limited range of plasma conditions. Therefore it is seldom possible to obtain direct information about all the degrees of freedom, and the experimentalist is often faced with the problem of estimating the complete state of a plasma from a limited number of measurements obtained over a few of the degrees of freedom. This extended interpretation can be made only through arguments of equilibrium which must be justified by theoretical considerations based on the relative rates of the reactions tending to drive the plasma either to or from equilibrium. Accordingly much of the time it is not possible to provide as complete a determination of the plasma state as is indicated in the above set.

If thermodynamic arguments are to be used in the extension of experimental data it is essential that at least one component have a Maxwellian velocity distribution and thus a meaningful temperature. Indeed the assumption of Maxwellian velocity distributions is required in the application of most of the diagnostic techniques. Often Langmuir probes can be used to verify the electron distribution. However, in the absence of such measurements one must justify the interpretation of experimental data with order of magnitude arguments concerning the thermal relaxation times. For the moderate temperature, optically thin plasmas being considered in this paper, the applied electric fields used in heating the plasmas are the primary cause of non-thermal energy distributions.* However, if the electron-electron relaxation time is short compared to the energy heating time, a thermal distribution will still exist to a close approximation. An identical criterion will hold for the ions. Since the neutrals are acted upon only by collisions with other particles and walls, they should not depart from a Maxwellian distribution. The electron-electron and ion-ion relaxation times can be estimated using Spitzer's "self-collision time" (Ref. 22). These relaxation times can also be used to estimate the time for species thermalization following the termination of a strong field. Similarly the time for equilibration of electron and ion temperatures can be estimated from Spitzer's "time of equipartition" (Ref. 22). Consider, for example, the following initial conditions which might exist following the electric discharge in argon in a moderate energy electric shock tube: $N_e = N_i = 10^{14}$ cm^{-3}, $T_e = 20{,}000$°K, $T_i = 1000$°K. The characteristic relaxation times in microseconds are $\tau_{ee} = 1{\cdot}2 \times 10^{-3}$, $\tau_{ii} = 3{\cdot}4 \times 10^{-1}$, and $\tau_{ei} = 48$.

* Strong shock waves are also considered in this paper. However, the time for achievement of a Maxwellian velocity distribution behind a strong shock wave is only a few mean collision times.

Thermal equilibration ($T_e = T_g$) will occur in the presence of an electric field when the rate of energy transfer from the highly mobile electrons to the relatively slow heavy particles is equal to the rate of energy transfer from the field to the electrons. This problem has been considered by Compton (Ref. 23), who has shown that if $E(\text{volts/cm})/P(\text{mm} - \text{H}_g) < 1$, then the equilibration criterion becomes (Ref. 24)

$$\frac{T_e - T_g}{T_e} = \frac{m_H}{8m_e}\left(\frac{eE_{\lambda e}}{3/2kT_e}\right)^2 \tag{4}$$

where m_H is the heavy particle mass and λ is the electron mean free path. Consider, for example, an argon plasma jet operating at atmospheric pressure with a field strength of 20 volts/cm (Ref. 25). If $T_e = 20{,}000°\text{K}$, equation (4) predicts $T_g = 19{,}600°\text{K}$ and to a first approximation the assumption of thermal equilibrium is justifiable. The problem of thermal equilibration is treated in more detail by Morse (Ref. 26).

Equilibration of bound electronic energy state populations is important in the interpretation of line emission spectroscopic data. Additional discussion of plasma thermodynamics can be found in Refs. 25 and 27 through 30.

Temperature measurements

Optical spectroscopy is probably the most effective method for determining plasma temperatures, although Langmuir probes are useful and other techniques such as microwave radiation (Ref. 12) have been used. Only spectroscopic methods in monatomic plasmas will be considered in this paper. The radiation in the absence of a strong magnetic field may be distinguished into three modes, each associated with different types of electron transitions between the various free and bound energy states within the plasma. Thus, one refers to line radiation, recombination radiation, and bremsstrahlung. The latter two form a continuous spectrum upon which the line spectrum is superimposed. Since the radiation is controlled almost entirely by the dynamics of the free electrons, absolute intensity measurements at best can provide information on the electron temperature only. Heavy particle temperatures can be determined only from the Doppler broadening of spectral lines, unless it can be shown by some other means that the electrons and the atoms or ions are at the same temperature.

Line radiation

Line radiation in a monatomic plasma occurs whenever there is a radiative transition between two discrete energy levels within an atom or ion. Consider the rate per unit volume R_{nm} at which atoms (or ions) undergo bound state transitions from the excited state n with energy E_n above the ground state to state m with energy E_m. The transition rate is given by:

$$R_{nm} = N_n A_{nm} + N_n B_{nm}\rho(\nu_{nm}) + [N_n \nu^e]_{nm} \tag{5}$$

where

$N_{n,m}$ = number of atoms (or ions) with electrons in the nth or mth excited state, cm^{-3}
A_{nm} = spontaneous transition probability, sec^{-1}
B_{nm} = stimulated transition probability, cm^3/ergs-sec^2
ν_{nm} = characteristic frequency of radiation between bound states E_n and E_m; $\nu_{nm} = (E_n - E_m)/h$, where h is Planck's constant
$\rho(\nu_{nm})$ = radiation energy density, ergs-sec/cm^3, and
ν^e = mean rate of collisional excitation or de-excitation of the level in question by collisions of atoms (or ions) with electrons, sec^{-1}

The first term on the right side of equation (5) corresponds to the spontaneous emission, the second to the stimulated emission and the last to de-excitation by electron collisions. Only the effect of electron collisions need be considered (see Section 3). A similar expression can be written for the rate of upward transitions from m to n, where spontaneous transitions are not included, since they cannot occur in the upward direction:

$$R_{mn} = N_m B_{mn} \rho(\nu_{nm}) + [N_m \nu^e]_{mn} \tag{6}$$

First consider the case of an optically thin plasma. The number of acts of spontaneous emission will greatly exceed the number of absorptions, which in turn will predominate over the number of stimulated emissions (Ref. 31). Thus,

$$N_n A_{nm} \gg N_m B_{mn} \rho(\nu_{nm}) > N_n B_{nm} \rho(\nu_{nm}) \tag{7}$$

From equation (5) the number of radiative transitions per unit time, per unit volume between the bound states n and m in an optically thin plasma is therefore $N_n A_{nm}$, and the intensity of the resulting spectral line is

$$I_{nm} = A_{nm} h \nu_{nm} N_n \tag{8}$$

Next we consider the case of an optically thick plasma in which radiative transitions are more important than collisional transitions and in which bound electronic state populations are in equilibrium with the radiation field. Thus

$$[N_{n,m} \nu^e]_{nm,mn} \ll N_n A_{nm},\ N_n B_{nm} \rho(\nu_{nm}),\ N_m B_{mn} \rho(\nu_{nm}) \tag{9}$$

According to the principle of detailed balancing, at equilibrium the number of upward transitions will equal the number of downward transitions (Ref. 74). Furthermore, the radiation field corresponding to the spectral line in question is assumed to maintain the bound state populations in a Boltzmann distribution at a radiation temperature which in laboratory plasmas is close to the electron temperature (Ref. 33). Thus, when equation (9) is combined with equations (5) and (6), the relation $R_{nm} = R_{mn}$, the Boltzmann relation, and the Einstein relations $g_n B_{nm} = g_m B_{mn}$ and

$A_{nm} = (8\pi h\nu^3/c^3)B_{nm}$, the following expression is obtained for the radiation intensity in the plasma at the frequency ν_{nm}:

$$\rho(\nu_{nm}) = \frac{8\pi h {\nu_{nm}}^3}{c^3}\left[\exp\left(\frac{h\nu_{nm}}{kT_e}\right) - 1\right]^{-1} \tag{10}$$

Thus, we see that the effect of a strong self-absorption is to trap radiation within the plasma until in effect the narrow spectral line is converted into a "rectangular" emission spectrum with a maximum amplitude that approaches the Planck value at the electron temperature.

The spectral line reversal method

The spectral line reversal method is essentially a simple method of calibration for making line intensity measurements over a limited intensity range. It was noted in the discussion of equation (10) that the effect of strong self-absorption of the radiation associated with a given spectral line is to make the line radiation intensity approach the Planck value. Thus to implement the reversal method an additive with a strong resonant line or lines is added to the plasma. Sodium is commonly used because of the very strong D-lines. A calibrated continuous spectrum light source such as a tungsten ribbon filament lamp is mounted with appropriate lenses and used to raise the plasma radiation level over the frequency range of the resonant line. This causes radiation transitions to dominate and the spectral line intensity is given by equation (10). The light source is viewed through the plasma with a spectrometer. If the brightness temperature of the source is greater than that of the resonant line, the resonant line will appear as a dark absorption line against the continuous background. If, however, the effective resonant line emission temperature is greater than that of the source, it will appear as a bright line superimposed on the continuum. At the reversal point the emission temperature of the gas is the same as the brightness temperature of the background, and the resonance line just disappears.*

The reversal temperature provides information on the processes which control the population of the bound state by quenching any attempts of the radiation field to surpass the appropriate kinetic temperature. In the monatomic plasma of interest in the paper the reversal method yields the electron temperature. In many studies in molecular gas mixtures it provides information on, for example, the vibrational or rotational temperatures.

The reversal method is limited to moderate temperature plasmas because of the limitations in the brightness temperatures of available continuum light sources (i.e. tungsten 2900°K, carbon arc 3600°K). We have found the method useful for temperature measurements in plasma electrical conductivity experiments, which were conducted with propane-air flame gases seeded with aqueous solutions of alkali metal compounds (Ref. 34), and for measurements in the expanded plasmas used in magnetoaerodynamic

* The reversal method depends on Kirchhoff's law, which states that at any wavelength the emissivity is equal to the absorption coefficient. According to Kirchhoff's law, at the reversal point no line is seen because at the resonant frequency the plasma is emitting as much energy as it is absorbing.

studies (Ref. 35). Although the reversal method was originally used for measuring temperatures in flames (Ref. 36), it has been used in other laboratories for shock tube work (Ref. 37) and recently for moderate-temperature non-equilibrium plasma conductivity experiments (Ref. 38), i.e., $T_a = 1600°K$, and $T_e = 2200°K$. For additional discussion of line reversal methods see Refs. 36 and 39.

Spectral line emission methods

Most laboratory plasmas are optically thin in the visible region except at the strong resonant lines. Accordingly line emission spectroscopy is a very useful diagnostic technique, particularly for determining the electron temperature. Its primary limitation is the requirement of thermal equilibrium among the upper bound states from which the measured spectral lines originate.

The radiant intensity emitted from a unit volume of an optically thin plasma—by an emission spectrum line corresponding to the transition from a state of higher energy n, with population density N_n, to a state of lower energy m—was given by equation (8). The spontaneous transition probability A_{nm} can be accurately calculated for hydrogen lines or lines from ions possessing just one residual electron. For other cases they must be determined by approximate calculations or experimentally. Reference (40) contains an excellent review of available transition probability data. Fortunately, considerable data are available for the atom and ion lines of the gases commonly used in the laboratory.

If line emission spectroscopy is to be a useful tool for electron temperature measurements, N_n must be related to T_e. The ion and atom bound electronic states are populated and de-populated by electron and heavy particle collisions, and radiative transitions. In optically thin plasmas collisional processes tend to dominate. Furthermore, the probabilities for excitation, de-excitation and ionization by electron collisions are much greater than for heavy-particle collisions. Thus, it is possible at certain conditions of electron density and temperature for the electron collisional processes to dominate and result in a thermal equilibrium of the free and bound state populations at the electron temperature. These conditions have been considered by several investigators (Refs. 41, 42, 43, and 44). In general, radiative depopulation effects will be greatest at the lower principal quantum numbers, while, due to the decreasing difference between energy levels, the collisional processes become increasingly important at the higher quantum numbers. Thus, one can define a principal quantum number $\bar{n}$ corresponding to a "thermal limit" (Ref. 41) above which the bound population distribution is Boltzmann and below which radiation effects are important. For low electron densities, the thermal limit is very close to the ionization limit. However, as the electron density increases and collisional excitation, de-excitation, ionization and recombination processes become more important, the thermal limit drops lower and lower, until at sufficiently high electron densities it reaches the ground level and all energy states have a Boltzmann population.

Wilson (Ref. 41) and Griem (Ref. 42) have derived approximate expressions for the thermal limit as a function of the electron density and temperature. Their expressions give essentially identical results and show that the thermal limit is a strong function of the electron density and a weak function of the temperature. For example, Griem obtains

$$N_e \geq 9{\cdot}2 \times 10^{17} Z^7 \left(\frac{kT_e}{X}\right)^{1/2} \left(\frac{E_2 - E_1}{X}\right)^3 \text{cm}^{-3} \tag{11}$$

for the electron density required for the thermal limit to include the ground state. Z is the charge number seen by the excited electron; i.e., $Z = 1$ for neutrals, $Z = 2$ for singly ionized atoms, etc. X is the ionization potential.* Typical conditions for a 1 ev hydrogen plasma are $N_e \sim 10^{15}$ cm^{-3} for $\bar{n}$ corresponding to the first excited state and $N_e \sim 10^{17}$ cm^{-3} for $\bar{n}$ extending to the ground state. Thus, it is seen that while very large electron densities are required for collision domination to extend to the ground state, moderate densities easily obtainable in the laboratory are sufficient to extend a Boltzmann distribution through the first excited state.

Griem (Ref. 42) has also derived similar expressions for the characteristic times required for the bound state populations to come into equilibrium and for the average distances through which atoms diffuse during these times.

When the thermal limit includes the ground state, the free states are populated according to the Saha equation, written here for atoms and first ions,

$$\frac{N_e N_i}{N_a} = 2\left(\frac{2\pi m_e k T_e}{h^2}\right)^{3/2} \frac{Q_i}{Q_a} \exp\left(-\frac{X}{kT_e}\right), \tag{12}$$

and the bound states according to the Boltzmann distribution, written here for atomic states:

$$\frac{N_n}{N_a} = \frac{g_n \exp\left(-\dfrac{E_n}{kT_e}\right)}{\sum\limits_m g_m \exp\left(-\dfrac{E_m}{kT_e}\right)} = \frac{g_n}{Q_a} \exp\left(-\frac{E_n}{kT_e}\right). \tag{13}$$

To a close approximation the electron temperature is the appropriate temperature in both distributions. Q_a and Q_i are the internal partition functions of the atom and ion. E_n and E_m are the energies and g_n and g_m are the statistical weights of the nth and mth bound states in the atom or ion. X is the effective ionization potential, corrected for plasma microfields (Ref. 45). The partition functions involve a summation over all the energy states and thus are strictly applicable only when all of these levels are populated at a well-defined electron temperature. If the thermal limit does not

* The condition imposed by equation (11) for thermal equilibrium can be relaxed by about a factor of 10 if the resonance line is optically thick.

extend to the ground level, equation (13) can be limited to the upper levels and written as

$$\frac{N_n}{N_m} = \frac{g_n \exp\left(-E_n/kT_e\right)}{g_m \exp\left(-E_m/kT_e\right)} \tag{14}$$

and a modified Saha equation can be written for a restricted system consisting of the free states and the bound states above the thermal limit, if ion excitation is neglected so that the ion partition function can be approximated by the statistical weight g_i of the ground state. This equation, which relates the population of the nth level of a given species to the electron density and the ground state population of the next higher ionization stage, is

$$N_n = N_e N_i \frac{g_n}{g_i} \frac{1}{2} \left(\frac{h^2}{2\pi m_e k T_e}\right)^{3/2} \exp\left(\frac{X - E_n}{kT_e}\right) \tag{15}$$

Equations (12) through (15) can be used to relate N_n to T_e in equation (8). For example, if the thermal limit extends to the ground state, equation (13) can be combined with (8) to give the following equation relating the absolute atom line intensity to the global atom density and the electron temperature:

$$I_{nm} = A_{nm} h\nu_{nm} N_a \frac{g_n}{Q_a} \exp\left(-E_m/kT_e\right) \tag{16}$$

A similar expression can be written for an ion line.

The partition function and the number density drop out of the intensity ratio for two spectral lines originating from the upper states, e.g., u and v, of a common species.

$$\frac{I_{nm}}{I_{uv}} = \frac{A_{nm}}{A_{uv}} \frac{\nu_{nm}}{\nu_{uv}} \frac{g_n}{g_u} \exp\left(\frac{E_u - E_n}{kT_e}\right) \tag{17}$$

Equation (17) requires that the thermal limit extend only through the energy states u and v. If one obtains a simultaneous intensity measurement of a series of lines from a given species, a graph of $\log\left(1/Ag\right)$ versus E will provide a straight line with slope $-1/kT_e$ if the bound states are indeed in thermal equilibrium (Ref. 46). This method therefore provides a check of the equilibration as well as a measure of the electron temperature (Ref. 44). Unfortunately, the corresponding energy levels within a given species are usually so close to each other that the intensity ratio is not a strong function of the temperature and the above procedures therefore rarely afford a sensitive temperature measurement except at rather low temperatures.

A more sensitive function of temperature can be obtained by using the form of the Saha equation (15) which relates the population N_n to the electron density and the ground state population of the next higher ion. Consider for example a neutral plasma composed of atoms and first ions. If it is assumed that the ions are primarily in the ground state,

$$I_{nm} = A_{nm} h\nu_{nm} N_e^2 \frac{g_n}{g_i} \frac{1}{2} \left(\frac{h^2}{2\pi m_e k T_e}\right)^{3/2} \exp\left(\frac{X - E_n}{kT_e}\right) \tag{18}$$

and if the electron density can be determined by, for example, the continuum emission or by microwave techniques, then equation (18) can be used, with a measurement of the absolute intensity I_{nm} of an atom line to determine the electron temperature.

A very strong function of temperature is obtained by using the intensity ratios of lines from subsequent ionization stages of the same element. Such a ratio, for example for an atom and ion line, will contain the term $N_a Q_i / N_i Q_a$, which can be eliminated using equation (12). The result,

$$\frac{I_{nm}{}^{i}}{I_{cd}{}^{a}} = \left[2 \frac{A_{nm}{}^{i}}{A_{cd}{}^{a}} \frac{g_n{}^{i}}{g_c{}^{a}} \frac{\nu_{nm}{}^{i}}{\nu_{cd}{}^{a}} \left(\frac{2\pi m_e k}{h^2}\right)^{3/2}\right] \frac{T_e{}^{3/2}}{N_e} \exp\left[\frac{-(X + E_n{}^{i} - E_c{}^{a})}{kT_e}\right] \quad (19)$$

is a strong function of temperature and a weak function of electron density throughout a large temperature range. For example, a 10 per cent uncertainty in the electron density will only result in approximately a 1 per cent error in temperature for the argon AI 4379 and AII 4158 lines in the range $T_e < 20{,}000°\text{K}$. Thus, for approximate temperature estimates one often can avoid absolute intensity measurements by simply using a step filter or photomultipliers to measure the relative line intensities and then guessing at the electron density. This method is also particularly desirable, because uncertainties in the transition probabilities and in the reduction of the ionization potential are negligible (Ref. 47). Also the partition functions drop out, thus relaxing the requirement that all excited states be in thermal equilibrium. Of course the states from which the lines originate must be in thermal equilibrium.

We have used the two-line method using atom and ion lines to estimate the thermodynamic state of the argon plasma generated in a conical type electromagnetic shock tube (Ref. 21). Time-resolved absolute intensity measurements were made by mounting six photomultipliers behind slits on the film plane of a Hilger Watts glass prism spectrograph. The photomultiplier lens and mirror system were designed so that with simple adjustments various combinations of spectral lines could be observed. The exit system was formed from a Kodak Type I-N 4 × 10 in. spectroscopic plate, using black lacquer base paint and the spectrum photographic image as a guide. The final wavelength adjustment of the slit system was made by rocking the prism while observing the photomultiplier output associated with an unshifted line from an argon discharge tube. The combined spectroscopic, photoelectric and lens systems were calibrated as a unit, using a previously calibrated tungsten ribbon-filament lamp and the tungsten data by Rutgers *et al.* (Ref. 48) and DeVos (Ref. 49). Equation (19) and equations of the form of equation (16) for the atom and ion line intensities were used to calculate N_e, N_a, and T_e from the absolute intensity data. The electron temperatures varied from 12,000 to 18,000°K, and peak electron densities from 10^{16} to 10^{17} cm^{-3}. At these electron densities, effects due to departures from thermal equilibrium should have been small compared to the experimental uncertainty. In general the temperature and number density data obtained from various combinations of the lines, and

the electron density data obtained from the absolute intensity of the continuum radiation and the Stark broadening of hydrogen impurity lines, were internally consistent within the expected experimental errors and uncertainty in the experimentally determined transition probabilities. The greatest deviations were found in low-pressure tests in which a high impurity level was observed.

Impurities in a laboratory plasma can be a cause of considerable grief, since they can completely change the kinetics of reaction processes. Also, they increase the number of components which must be identified for a complete specification of the thermodynamic state. However, impurities can be of use in bracketing the electron temperature in a high-temperature plasma, particularly if one has some idea of the electron density and can

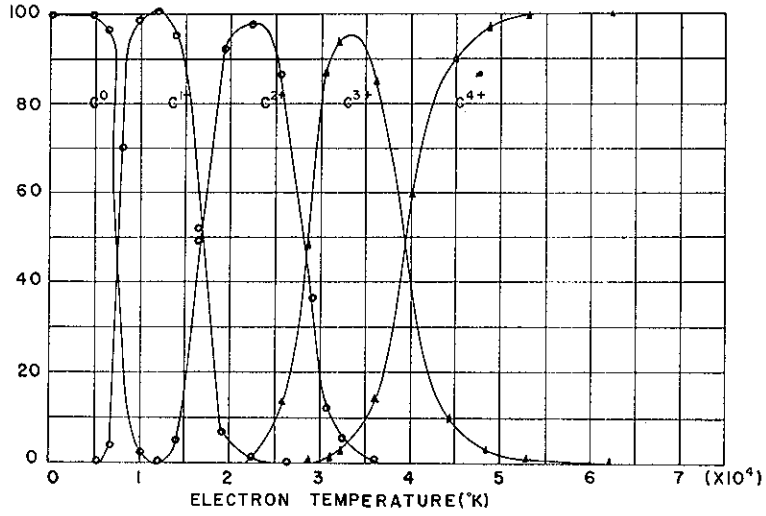

Fig. 3. Abundance of carbon ions vs electron temperature for n = 10^{14} *electrons/cm*^{3} *determined from Saha relation. From McNally, "The Direct-Current Experiment (DCX) and High-Temperature Measurements in the Carbon Arc" in* Optical Spectrometric Measurements of High Temperatures, *Ed. P. J. Dickerman, University of Chicago, 1961.*

justify the assumption of Saha equilibrium. Figure 3 is a plot of the set of Saha equations for the various ions of carbon as a function of the electron temperature and at a constant electron density. Such a plot can be used with a time-integrated spectrogram to estimate the maximum electron temperature in a device. For example, suppose a strong carbon third ion line is found on a spectrogram of the radiation from a laboratory device, and it is estimated that the electron density is about 10^{14} cm^{-3}. Furthermore, suppose that no strong carbon *2nd* ion or *4th* ion lines are found. From Fig. 3 we estimate that T_e must be between 3 and 3·75 eV. This is temperature determination to within about 25 per cent without an absolute intensity measurement.

The maxima corresponding to the various species concentrations in Fig. 3 are suggestive of another method which is frequently useful for optically thin radially symmetric plasmas. The method is applicable when the plasma is in complete thermal equilibrium and when the pressure throughout the plasma is constant and is known. Such a set of conditions often exists, for example, in an atmospheric plasma jet. Under these conditions it is useful to combine equation (16) with equation (12) and an equation expressing the total pressure as a function of the component partial pressures. The result yields the line intensity of the species in question as a function of the total pressure and the temperature. Thus, if the pressure is known, a measurement of the absolute intensity of one spectral line is sufficient to determine the temperature. Furthermore, for a given pressure the intensity goes through a maximum at a temperature T_M. Thus if the inner core of a radially symmetric plasma is hotter than T_M, the radial intensity distribution of the line in question will go through a maximum. At the maximum the absolute intensity will be known and the spectrometer will be effectively calibrated since it can be shown (Ref. 3) that for such a radially symmetric plasma

$$\frac{I(T)}{I(T_M)} = \frac{I(r)}{I(r_M)} \qquad (20)$$

$I(r)$ is the measured radial intensity distribution and is obtained using the solution to the Abel integral equation (Ref. 50) to invert analytically the experimental data, since the spectrograph measures the integrated distribution produced by the thermal gradient existing along the axis of observation. r_M is the radius at which T_M occurs, $I(T)$ is the theoretical intensity for atom line in question at temperature T and the appropriate pressure, and $I(T_M)$ is the intensity maximum for the appropriate pressure. Thus a measurement of $I(r)$ is sufficient to determine $T(r)$, the radial temperature distribution. This method has the advantage that the transition probability drops out of the ratio. Transition probabilities for many species are not known accurately. It must be noted that equation (20) does not hold and the method is not applicable unless the off axis peak in the line intensity is observed at some point in the plasma flow field. We have found this method very useful and have for example used the argon AI 4158 line to analyze a 4 kw plasma jet operating at atmospheric pressure (Ref. 3).

In this section we have considered the methods by which spectrum line intensity measurements can be used to determine the electron temperature. Although the final choice of a method in a given situation will depend on many factors, the following points should be considered. (a) Are the translational temperatures expected to be in equilibrium? (b) Are the bound atomic states expected to be in equilibrium? (c) Is the plasma optically thin at the wavelength of interest? (d) Are high-density corrections necessary? Although these corrections have not been emphasized in this paper, they can be important, and one such correction, the lowering of the ionization potential by plasma microfields, should be taken into account when using the Saha equation in dense plasmas ($N_e \sim 10^{15}$ cm^{-3}) if accuracy is desired. This and other high-density corrections are discussed in Ref. (45).

(e) What combination of line ratios, etc., will provide the most favorable relationship with temperature in the expected temperature range so that large errors in intensity will result in small errors in temperature? An excellent review of errors in plasma spectroscopy is given in Ref. (47).

Continuum radiation

The total continuum radiation emitted by the plasma is due to a combination of two types of radiative transitions involving the free electrons: the bremsstrahlung or free-free continuum, and the free-bound continuum which results from the radiative recombination of electrons with positive ions. The two types of radiation are superimposed to the extent that they cannot be separated experimentally.

An expression for the bremsstrahlung in the visible spectrum can be derived by considering classically the Coulomb collision of an electron and an ion. However, the free-bound transitions are more complex. There are two very useful ways of deriving the formula for the total emission. For hydrogen or hydrogen-like ions the equation is usually derived from the continuous absorption coefficients of single atoms, since these absorption coefficients can be calculated from quantum mechanics for one electron system (Ref. 45). The emission is then found by multiplication with the Kirchhoff-Planck function and correcting for stimulated emission. An expression for the emission in terms of the densities in the appropriate lower states results. These densities are then related to the densities in the free states via Boltzmann factors, equation (14), and the Saha equation (12). The result is a rather complex relationship giving the continuum emission as a function of the ion density and the electron temperature and density.

However, in most practical situations in gaseous discharges at low pressures, the number of acts of spontaneous emission greatly exceeds the number of stimulated emission (Ref. 31). Thus an approximate theory, which is very useful in analyzing experimental data, may be formulated by deriving spontaneous transition probabilities for free-bound and free-free transitions (Ref. 51). The only assumption of equilibrium which is required is that the free electrons are in a Maxwellian velocity distribution. In order to simplify the results, the free-bound problem is assumed to be similar to the free-free problem; i.e., the upper bound states of the atom are assumed to be so close together that they can be treated as a continuum. The final result is the same as that obtained by Unsöld (Ref. 52) for the continuum radiation per unit frequency:

$$\varepsilon_\nu = 5{\cdot}41 \times 10^{-46} Z_{\text{eff}}\, \bar{g}\, \frac{N_e N_i}{T_e^{1/2}} \text{ watts/cm}^3\text{-ster-sec}^{-1} \qquad (21)$$

Z_{eff} is the effective charge seen by the free electron, and $\bar{g}$ is approximately equal to one and is weakly dependent on the frequency. Equation (21) predicts a frequency independent spectrum and is applicable from the low frequencies up to a cut-off frequency defined by the energy interval between the effective ionization potential and the energy level below which the assumption of dense states is invalid. The more detailed theory (Ref. 45)

predicts that beyond the cut-off frequency the continuum falls off according to $\exp\left(-\frac{h\nu}{kT_e}\right)$. Superimposed on this generally decreasing continuum are peaks corresponding to the series limits for recombination into the lower isolated levels in the atom. This picture of the continuum frequency dependence has been observed experimentally, although the proportionality constant is in doubt for complex atoms. For example, Olsen (Ref. 53) found in argon at $N_e = 2 \times 10^{17}$ that lowering of the ionization potential shifted the cut-off frequency to about 10,000 Å. Between 10,000 Å and 6000 Å he found recombination peaks corresponding to transitions into the $2p$ states, and between 6000 Å and approximately 4300 Å there was a region of very weak frequency dependence in which the continuum was found to obey the function dependence of equation (21). This was followed by another region of recombination peaks for the $1s$ states and then a rapid reduction in the continuum intensity. We have used Olsen's data to obtain a proportionality constant for the argon continuum emission in the region between the $1s$ and $2p$ recombination peaks:

$$\varepsilon_\nu|_{(1s-2p)} \sim 8{\cdot}5 \times 10^{-46} \frac{N_e^2}{T_e^{1/2}} \text{ watts/cm}^3\text{-ster-sec}^{-1} \tag{22}$$

Equation (22) has been found to be consistent with results obtained from line emission and broadening measurements (Ref. 21).

The functional dependence of equation (21) limits its value for a direct determination of the electron temperature. The primary value of continuum measurements in temperature determinations is for use with the ratio of the atom line and continuum intensities. The continuum intensity I_c over a band $\Delta\lambda$ is equal to $\varepsilon_\nu c\,\Delta\lambda/\lambda^2$. Thus, equation (22) can be combined with equation (16) to form the ratio

$$\frac{I_{nm}}{I_c} = \frac{A_{nm}h\nu_{nm}}{BZ_{\text{eff}}^2\,\bar{g}\,(4\pi)}\frac{g_n}{g_i}\frac{1}{2}\left(\frac{h^2}{2\pi m_e k}\right)^{3/2}\frac{\lambda^2}{c\,\Delta\lambda}\,T_e^{-1}\exp\left(\frac{X-E_n}{kT_e}\right) \tag{23}$$

which is only a function of the electron temperature. B is the proportionality constant for the continuum relationship.

The continuum intensity is particularly effective in making electron density measurements and will be discussed in a later section.

Doppler broadening temperature measurements

The broadening of a spectral line may be broken into three classes according to the cause: natural line broadening, collision broadening, and Doppler broadening.

Doppler line broadening results when the emitting atoms or ions have a high-velocity component in the direction of the observer. When the spectroscopic observations are made perpendicular to the direction of fluid flow, only the thermal velocity will give rise to a Doppler effect, which provides the only spectroscopic method of direct determination of the heavy particle temperature. It can be shown that the Doppler broadening of a spectral

line due to the thermal motion of emitters with a Maxwellian velocity distribution is given by (Ref. 54)

$$2\Delta\lambda_D = 7{\cdot}16 \times 10^{-7}\lambda_0\sqrt{\frac{T}{m}} \tag{24}$$

where $\Delta\lambda_D$ is the observed Doppler half width of the broadened line in Å, λ_0 is the wavelength of the unperturbed line in Å, T is the translational temperature, and m is the molecular weight of the emitting species. In argon at 20,000°K, $2\Delta\lambda_D$ will be only ~0·07 Å at 4500 Å. Thus, in the high-density ($N_e \sim 10^{16}$ cm^{-3}) moderate temperature (~30,000°K) plasmas normally encountered in the laboratory, Doppler broadening is of little use, since it will be overshadowed by collision broadening. However, in the high-temperature moderate density thermonuclear plasmas Doppler broadening will dominate and is a useful diagnostic tool.

Spectroscopic methods for electron density measurement

Spectroscopic methods were discussed previously in connection with temperature measurements. In this section we briefly consider the application of optical spectroscopic methods to the determination of the electron density.

The electron density can be determined from the measurement of the absolute intensity of a first ion line, so long as the second ionization is small (see equation (16)). The partition function in equation (16) requires that the bound states be in complete equilibrium. However, at moderate temperatures this error will be small if the upper states are in equilibrium, since the partition function will be determined by the statistical weight of the ground state, and the electron density will be practically equal to the density of ions in the ground state. At lower temperatures, if the temperature is known, the electron density can be determined from the absolute atom line intensity using equation (18).

As was mentioned in the section on continuum radiation the electron densities may be determined from the absolute continuum intensity in that part of the spectrum where the continuum is nearly independent of frequency. In this region the continuum intensity given by equation (21) is a weak function of temperature and a strong function of the electron density. Also equation (21) is only weakly dependent on equilibrium requirements beyond a Maxwellian velocity distribution for the electrons. Furthermore, the electron density will depend on only the square root of the proportionality constant. Thus if the temperature can be estimated, equation (21) is a useful tool for determining the electron density.

Collision broadening occurs because the emitter suffers a collision which disturbs the emission mechanism, by dividing the wave of emitted radiation into incoherent wave trains or by shifting the energy levels of the emitter by a Stark effect. Stark broadening, which is nearly independent of temperature but is strongly dependent on the ion density and the level of ionization, is most important in highly ionized plasmas (~10^{16} cm^{-3}) of current

engineering interest and provides a very useful means of determining the electron density.

Griem (Ref. 47) has calculated the Stark profiles for a number of hydrogen and helium lines, considering the contributions of both the electrons and ions. The accuracy of the calculation is estimated to be about 10 per cent. The Stark broadening is a strong function of electron density and a very weak function of temperature in the range of his calculations, 5,000–40,000°K. Also, assuming charge neutrality and only first ionization, the Stark profiles are independent of the ion species present, and his results therefore apply equally well to hydrogen mixtures. We have found measurements of the Stark broadening of the hydrogen H_β line, which originated from hydrogen impurities in an argon plasma, to be very useful in complementing other spectroscopic measurements. The Griem theory was used for the calculations. Griem (Ref. 55) has also compiled useful working data for argon and cesium.

PLASMA-ELECTROMAGNETIC WAVE INTERACTIONS

Previously we mentioned the disadvantages of introducing probes into the plasma flow. In the preceding section we described spectroscopic techniques which circumvent this problem because they rely on radiations emanating from the plasma. We shall now discuss another type of diagnostics which does not perturb the flow. Thus we consider the propagation of electromagnetic waves through the plasma and subsequent investigation of the change in propagation characteristics due to the presence of the plasma. Although the theory is generally applicable, in our laboratory studies we deal in the microwave regime.

Because the rigorous analytical formulation of such diagnostics is very complex we use a highly simplified model which nevertheless provides acceptable information. In particular we consider only elastic collisions (Ref. 56) and in the following two sections we study the motion of a statistically average delectron in an unbounded, homogeneous plasma. Two cases can be treated: isotropic and anisotropic plasmas.

Homogeneous isotropic plasmas

The average electron formulation assumes that the average drift velocity of an electron in the plasma defines the current per particle. The equation of motion for the average electron is

$$\frac{d\vec{V}_e}{dt} + \nu_{eff}\vec{V}_e = -\frac{e}{m_e}\vec{E}_0 \exp(j\omega t) \tag{25}$$

where we have assumed a harmonic time dependence for the electric field. $\vec{V}_e$ is the average drift velocity and the term ν_{eff} in the damping term is an "effective" collision frequency of the average electron with heavy particles and is assumed to be independent of electron energy.

To calculate the collision frequency rigorously, it is necessary to know

the composition of the plasma, the electron velocity and the collision cross-section of all constituents that contribute to the total electron collision probability. We will retain the ν_{eff} formulation since little error is introduced by using this simplified approach (Ref. 57). From the steady-state solution of equation (25) and defining the current density as the product of charge density and average velocity, one obtains

$$\vec{J} = \frac{e^2 N_e \vec{E}}{m_e(j\omega + \nu)} \tag{26}$$

where we now write ν for ν_{eff}.

Equation (26) consists of a current both in and out of phase with the applied electric field and by analogy with the Maxwell equations we now define a plasma conductivity

$$\sigma = \frac{e^2 N_e \nu}{m_e(\nu^2 + \omega^2)} \tag{27}$$

and a plasma dielectric constant

$$\varepsilon = \varepsilon_0 \left(1 - \frac{e^2 N_e}{m_e(\nu^2 + \omega^2)}\right) \tag{28}$$

In terms of the electron plasma frequency ω_p, the constitutive parameters are

$$\sigma = \frac{\varepsilon_0 \omega_p^2 \nu}{\nu^2 + \omega^2} \tag{29}$$

$$\varepsilon = \varepsilon_0 \left(1 - \frac{\omega_p^2}{\nu^2 + \omega^2}\right) \tag{30}$$

Alternatively the plasma may be treated as a medium characterized by an effective dielectric coefficient given by the following:

$$\begin{aligned} K &= K_r - jK_i \\ K_r &= 1 - \frac{\omega_p^2}{\omega^2 + \nu^2} \\ K_i &= \frac{\omega_p^2}{\omega^2 + \nu^2}\left[\frac{\nu}{\omega}\right] \end{aligned} \tag{31}$$

These formulations of the problem permit plane transverse solutions to the wave equation of the form,

$$\begin{aligned} \vec{\psi} &= \vec{\psi}_0 \exp(j\omega t) \exp(-j\beta_0(\vec{n} \cdot \vec{r})) \\ &= \vec{\psi}_0 \exp(j\omega t) \exp(-(\alpha + j\beta)r) \end{aligned}$$

where: $\vec{\psi}$ represents either the electric or magnetic field

$\vec{\psi}_0$ is the amplitude of either the incident electric or magnetic field

$\vec{n}$ is the refractive index of the plasma

$\vec{r}$ is the position vector

β_0 is the free space wave number or phase constant

α, β are the attenuation and phase constants respectively of the plasma

The approach that is followed is a matter of taste and convention. Thus when dealing with optical frequencies, the index of refraction is usually used while the propagation constant approach is used in the microwave region of the electromagnetic spectrum.

In an unbounded, homogeneous, isotropic plasma, electromagnetic wave propagation will be governed by the refractive index (or dielectric coefficient), the real part of the refractive index determines the phase variation and the imaginary part the amplitude variation or attenuation. In terms of the effective dielectric coefficient, we have

$$\alpha/\beta_0 = \sqrt{\frac{|K| - K_r}{2}} \qquad \beta/\beta_0 = \sqrt{\frac{|K| + K_r}{2}} \tag{33a, b}$$

$$n = K^{1/2} = \frac{\beta + j\alpha}{\beta_0} \qquad |K| = (K_r^2 + K_i^2)^{1/2}$$

For a lossless plasma, $\nu \to 0$, the electrical conductivity $\sigma \to 0$ and only the ratio ω_p/ω determines the nature of the wave motion within the plasma. As $\omega_p/\omega \to 1$, the lossless phase constant, $\beta = \omega\sqrt{\mu_0\varepsilon} \to 0$ and wave propagation does not exist.

One may solve for the individual propagation coefficients α and β obtaining for the slightly lossy plasma ($\nu^2 \ll \omega^2$)

$$\alpha \cong \frac{\beta_0}{2}\left[\frac{\omega_p^2/\omega^2(\nu/\omega)}{(1 - \omega_p^2/\omega^2)^{1/2}}\right] \tag{34}$$

$$\beta \cong \beta_0\left[1 - \frac{\omega_p^2}{\omega^2}\right]^{1/2} \tag{35}$$

From these two equations it is apparent that if the propagation coefficients, α and β, are known one can solve for the plasma frequency, and consequently the electron density, and the effective electron collision frequency can be obtained. It is to be understood that the electromagnetic frequency is assumed to be greater than the plasma frequency ($\omega > \omega_p$).

In considering electromagnetic wave propagation in a plasma part of the incident energy is reflected, while part is absorbed and attenuated by the plasma and the rest is transmitted through the plasma, if we assume normal incidence upon an unbounded slab of plasma and neglect scattering. The total reflected and transmitted fields may be determined by an analysis based upon multiple reflections in the slab and subject to certain reasonable simplifying assumptions (Ref. 56). Thus, it is possible to calculate the attenuation constant α and phase constant β, from a knowledge of these reflection and transmission coefficients and hence σ and ε or ω_p and ν_{eff}.

A second approach for determining the attenuation and phase constants involves the transmission of electromagnetic waves through the plasma and measuring the phase change and attenuation of the transmitted waves. The data are reduced to values of α and β by assuming that reflections at

the plasma-air interface do not affect the observation. If d is the width of the plasma, the observed change in phase $\Delta\Phi$ is

$$\Delta\Phi = (\beta_0 - \beta)\,\mathrm{d} \tag{36}$$

Similarly, the observed change in attenuation, $\Delta\alpha$ is

$$\Delta\alpha = \alpha\,\mathrm{d} \tag{37}$$

Thus, a measurement of $\Delta\Phi$ and $\Delta\alpha$ lead to α and β, and consequently to the electron density and effective collision frequency.

Homogeneous anisotropic plasmas

We consider next the propagation of a plane electromagnetic wave incident normally upon a slab of homogeneous anisotropic plasma. Again the plasma is considered to be a plane of finite thickness in the direction of propagation, but otherwise infinite in extent. However, the constitutive parameters are no longer scalars, but tensors due to the assumed anisotropy.

The conventional formulation of the constitutive parameters is again based upon the assumption that the average drift velocity of an electron in the plasma defines the current per particle and obeys the equation of motion

$$\frac{d\vec{V}_e}{\mathrm{d}t} + \nu\vec{V}_e = -\frac{e}{m_e}(\vec{E} + \vec{V}_e \times \vec{B}) \tag{38}$$

where ν again represents the effect of collisions.

Assuming that the static magnetic field is directed along the z-axis and recalling generally that $\vec{J} = \vec{\vec{\sigma}} \cdot \vec{E}$, the steady-state solution and expansion of equation (38) leads to

$$\vec{\vec{\sigma}}_z = \begin{pmatrix} \sigma_1 & \sigma_2 & 0 \\ -\sigma_2 & \sigma_1 & 0 \\ 0 & 0 & \sigma_3 \end{pmatrix} \tag{39}$$

where

$$\sigma_1 = \frac{\varepsilon_0\omega_p{}^2(\nu + j\omega)}{(\nu + j\omega)^2 + \omega_c{}^2} \tag{40a}$$

$$\sigma_2 = \frac{\varepsilon_0\omega_p{}^2\omega_c}{(\nu + j\omega)^2 + \omega_c{}^2} \tag{40b}$$

$$\sigma_3 = \frac{\varepsilon_0\omega_p{}^2}{\nu + j\omega} \tag{40c}$$

The preceding formulation of the constitutive parameters incorporates the effect of the charge carriers in terms of a conductivity tensor while the dielectric constant is that of free space, namely ε_0. (Alternatively, the constitutive parameters could have been developed in terms of a dielectric tensor and zero conductivity. Either approach may be used to advantage.) Thus, the existence of the static magnetic field serves to replace the scalar

constitutive parameters by tensors, and the boundary value problem reduces to solving Maxwell's equations in the following form.

$$\nabla \times \vec{H} = (\vec{\sigma} + j\omega\varepsilon_0)\vec{E} \tag{41}$$

$$\nabla \times \vec{E} = -j\omega\mu_0\vec{H} \tag{42}$$

We have shown that the effect of an applied d.c. magnetic field upon an initially homogeneous, isotropic plasma is to induce a tensor form for the constitutive parameters thus rendering the plasma anisotropic. We will next examine how electromagnetic waves propagate through such a medium. We recognize three cases of interest, (a) the propagation vector is collinear with the static magnetic field; (b) the propagation vector is perpendicular to the magnetic field; and (c) the propagation vector and the magnetic field are inclined to one another. The first and second cases are particularly important, and we shall discuss them further. The former case we shall call longitudinal propagation and the latter transverse propagation.

Longitudinal propagation

For the longitudinal case, we seek a solution to Maxwell's equations with a propagation term $e^{j\omega t-\gamma z}$ with a tensor conductivity given by equation (39). Insertion of these assumptions into Maxwell's equations yields the following expression for the propagation constant.

$$\gamma = j\omega\sqrt{\mu_0\varepsilon_0}[1 - j\sigma_1/\omega\varepsilon_0(1 \mp j\sigma_2/\sigma_1)]^{1/2} \tag{43}$$

It should be noted that there are two possible values for the propagation constant depending upon the sign of the term in the bracket. The $\pm$ signs indicate the decomposition of the original plane wave into two contra-rotating circularly polarized waves with different propagation coefficients.

$$\gamma_\mp = \alpha_\mp + j\beta_\mp \tag{44}$$

It can be shown by separating the equations into real and imaginary parts and again using the slightly lossy approximation that

$$\beta_\mp = \beta_0\left[1 - \frac{\omega_p^2}{\omega^2}\left(\frac{1}{1 \pm \omega_c/\omega}\right)\right]^{1/2} \tag{45}$$

$$\alpha_\mp = \frac{\beta_0}{2}\left[\frac{\omega_p^2/\omega^2(\nu/\omega)}{(1 \pm \omega_c/\omega)^2\left(1 - \dfrac{\omega_p^2/\omega^2}{1 \pm \omega_c/\omega}\right)^{1/2}}\right] \tag{46}$$

We have seen that as a result of the presence of the static magnetic induction, the plasma exhibits the features of a double refracting medium. If one investigates the propagation of electromagnetic waves through such a plasma, one finds that the plane of polarization of an initially linearly polarized wave is rotated as the wave propagates through the plasma and that the angle of rotation is given by

$$\theta = \left(\frac{\beta_+ - \beta_-}{2}\right) \mathrm{d} \tag{47}$$

where $\beta_{\pm}$ are given by equation (45) for the slightly lossy plasma and d is the thickness of the plasma in the direction of propagation. Furthermore, because of the different attenuation constants of the two circularly polarized components, the resultant wave is elliptically polarized with an ellipticity

$$\xi = \frac{e^{-\alpha_+ z} - e^{-\alpha_- z}}{e^{-\alpha_+ z} + e^{-\alpha_- z}} = \tanh(\alpha_- - \alpha_+)\, d/2 \tag{48}$$

These phenomena are the well-known Faraday rotation and ellipticity of optics. It is evident that the Faraday rotation angle depends directly upon the static magnetic field, the plasma electron density and the distance of propagation of the electromagnetic wave in the plasma. It is also important to realize that even a small collision frequency ($\nu/\omega \geq 0{\cdot}01$) can influence the Faraday rotation significantly for certain combinations of electron density and magnetic field strength.

Transverse propagation

The second important case of electromagnetic wave propagation in an anisotropic plasma is when the propagation vector is perpendicular to the magnetic field or the so-called transverse propagation. We will continue to assume that the wave propagation is in the z-direction, but let the static magnetic field be oriented in the y-direction. Insertion of these assumptions into Maxwell's equations and expansion yields two modes of propagation or two values of the propagation constant. One mode arises when the exciting electric field (E_x) is perpendicular to the static magnetic field and is given by

$$\gamma_{\perp} = j\beta_0 \left[\frac{(1 + j\omega\varepsilon_0/\sigma_1)^2 + (\sigma_2/\sigma_1)^2}{(j\omega\varepsilon_0/\sigma_1)(1 + j\omega\varepsilon_0/\sigma_1)}\right]^{\frac{1}{2}} \tag{49}$$

An analysis of equation (49) indicates that this mode exhibits cut-off and resonance properties similar to the γ_+ wave of the longitudinal propagation study of the previous section.

For the other mode, the electric field is parallel to the static magnetic field and the propagation constant is given by

$$\gamma_{\parallel} = j\beta_0[1 - j\sigma_3/\omega\varepsilon_0]^{1/2} \tag{50}$$

$\gamma_{\parallel}$ is not a function of the magnetic field and is equivalent to the propagation constant of the homogeneous isotropic plasma. Because this mode of propagation is not affected by the magnetic field, the name ordinary wave has been applied to it, thus leading to the term extraordinary wave for the other mode.

One also finds for transverse propagation that the resultant field is rotated and elliptically polarized (Ref. 56). The difference between the longitudinal and transverse cases will be discussed next. In the former we have the rotation of the plane of polarization or the Faraday effect as the most significant result. The effect of losses is to induce elliptical polarization with some alteration of the orientation, depending upon the magnitude of the losses. In the transverse case, the Cotton-Mouton effect of optics, we have the

degeneration of plane polarization into elliptical polarization even without losses. The effect of losses is not only to change the ellipticity but also to alter the orientation. Another important difference is the effect of the direction of the static magnetic field; a reversal of the magnetic field reverses the direction of the Faraday effect, but does not alter the Cotton-Mouton effect.

Inhomogeneous plasmas

Thus far we have assumed that the plasma is homogeneous. Because the dependability of any measurement technique will be primarily affected by how well the plasma under consideration satisfies the assumptions governing the theoretical plasma model, we review briefly propagation in an inhomogeneous plasma.

The principal difference between propagation in homogeneous and inhomogeneous plasma is the dependence of the latter constitutive parameters upon position. Thus, the propagation of electromagnetic waves in inhomogeneous plasmas is marked by an exceptionally great variety of possibilities in the choice of the spatial dependence of the constitutive parameters. As might be expected, the appropriate wave equation has no general solution in terms of known functions for an arbitrary functional dependence upon position; however, particular cases of some practical importance can be solved. One detailed theoretical study of the effect of electron density gradients in the direction of propagation has been carried out by Albini and Jahn (Ref. 58). It was shown that the propagation of electromagnetic waves through the plasma is primarily affected by the thickness of the transition zone (in the direction of propagation) rather than the shape of the zone. The properties of the propagating wave (reflection and transmission coefficients) can be strongly influenced by these transition zones if the thickness of the zone is greater than a few tenths of a wavelength. Obviously, then, the use of high electromagnetic wave probing frequencies, otherwise advantageous from the viewpoint of spatial resolution, tends to aggravate this situation.

In free space transmission measurements involving the measurement of phase charge, the plasma phase constant β given by equation (35) is now a function of position and the phase shift is given by

$$\Delta\Phi = [\beta_0 - \beta(z)]\, \mathrm{d} \tag{51}$$

Wharton and Slager (Ref. 59) calculated the phase shift for various assumed electron density distributions and devised a method for experimentally determining the electron density profiles using a microwave interferometer scheme to measure the phase shift due to the plasma at three or more microwave probing frequencies. Thus, an estimate of the electron density profile can be obtained. However, the experimental arrangements can become quite complicated due to the necessity of making microwave measurements at several different frequencies.

The most promising approach for studying an inhomogeneous, anisotropic plasma appears to be contained in the functional dependence of the Faraday

rotation angle upon the electron density distribution in the direction of propagation for the lossless case and longitudinal propagation. The Faraday rotation of the plane of polarization that results due to the inhomogeneous anisotropic plasma is given by

$$\theta = \frac{\beta_0}{2} \int_0^d [\beta_+(z)/\beta_0 - \beta_-(z)/\beta_0] \, dz \tag{52}$$

The integration of equation (52) is in general difficult, however. Warder and Hector have carried through the integrations for various assumed electron density distributions, i.e., cosine, parabolic, Gaussian and trapezoidal distributions (Ref. 60). These results have a twofold usefulness. First, it is possible to determine the electron density profile of a plasma in a magnetic field when one cannot orient the electric field vector parallel to the direction of the magnetic field. Secondly, instead of determining the propagation phenomena as a function of microwave frequency, one can vary the magnetic field strength. Generally this is easily done and also allows a wider range of parameters to be covered than when only the microwave frequency is changed.

Effects due to finite plasmas

Thus far we have considered the propagation of electromagnetic waves in unbounded plasmas and found that one can obtain information about the electron density and collisional processes from a knowledge of the change in the wave propagation characteristics due to the presence of the plasma. Many of the plasmas encountered in situations of practical interest are not actually unbounded and introduce certain complications. On the other hand, such finite boundary plasmas offer the possibility of different methods of determining plasma properties and some of these methods will be discussed next.

In addition to the effect of reflections at plasma-interfaces which were mentioned earlier, two other important effects are those of refraction and diffraction. Because the index of refraction of a plasma ($n = K^{1/2}$) differs in general from that of its surrounding medium and has a value of less than one, refraction will occur at any interface where the angle of incidence of an electromagnetic wave differs from zero. This feature, in addition to the fact that the plasma has a refractive index of less than unity and possibly playing the role of a lens in defocusing the microwave beam, makes it desirable to maintain the microwave beam normal to any interfaces of interest in most experimental arrangements.

Because the size of many laboratory plasmas is of the order of a free-space wavelength, it is also important to consider diffraction effects. To allow solution of these problems, it is necessary to specify the geometry of the plasma, the spatial variation in the plasma properties and the nature of the incident wave front. For simple geometric shapes such as cylinders, one may treat the problem as a scattering problem (Refs. 61 and 62) where the incident electromagnetic field is a plane wave and the scattered field possesses

circular symmetry. Thus, it is possible to apply the usual boundary conditions and obtain a solution. In principle it is also possible to obtain the electron density distribution by measuring the diffraction pattern as proposed by Shmoys (Ref. 63).

Microwave measurement methods

As a result of the mathematical development of the previous section, we have seen that it is possible to obtain information concerning the electron density and effective electron collision frequency of plasmas by observing the change in some propagation phenomena of the electromagnetic wave interacting with the plasma. With the use of microwaves, it is generally easy to satisfy the condition that $\nu^2 \ll \omega^2$. Hence, the fundamental limitation on the use of microwaves is that the critical plasma frequency be less than the probing microwave frequency.

From the viewpoint of plasma diagnostics, one can classify microwave techniques into two broad categories. The first of these involves bounded wave propagation where the plasma is usually placed in a wave guide or resonant cavity. The cavity method of determining the plasma electrical properties will generally not be applicable for studying the plasmas encountered in energy conversion and propulsion devices. This is due to the high-charge densities and large size and various geometrical configurations which are encountered.

Another method of using guided-wave propagation in determining plasma properties are experiments (Refs. 64 and 65) with shock-heated plasmas, with the shock wave actually passing through a specially designed section of the waveguide. These experiments indicate the change in the transmitted and reflected wave characteristics caused by the plasma flow. Still other methods include the experiments performed using the shock tube itself as a waveguide (Ref. 66). In these experiments, the microwaves are propagated axially along the shock tube and interact with the oncoming shock wave. By measuring the amount of the microwave power reflected by the shock wave, and assuming an electron density distribution behind the shock wave, the collision frequencies of the electrons with the other constituents of the plasma and ionization processes may be studied. As was mentioned previously, these guided-wave techniques are of limited usefulness in many applications, particularly those involving high-temperature steady-flow facilities where one encounters deleterious material effects even if the flow configuration is amenable to microwave techniques. Of particular attractiveness for the diagnostics of plasma flow facilities are the free-space propagation schemes which have been applied to shock tubes (Ref. 67), plasma jets (Ref. 68), and high-frequency electrodeless discharge tunnels (Ref. 69).

Excluding the scattering and radiation methods mentioned previously, these free-space propagation techniques involve measurements of either transmission or reflection of electromagnetic waves incident upon the plasma. Using a suitable theory such as that presented in the previous section, one then relates the microwave data to the plasma properties. Generally one

measures the change in phase and amplitude of the microwave signal due to the presence of the plasma, although when a magnetic field is present one may measure the polarization of the microwave field (i.e., Faraday rotation) to deduce the plasma properties.

Although it is desirable to be able to probe the plasma with good temporal and spatial resolution, microwave techniques suffer from poor spatial resolution being limited to distances of the order of the microwave wavelength employed. Microwave techniques suffer another inherent limitation in that the microwave frequency must be matched closely to the electron plasma frequency which then dictates the wavelength that must be used. It also should be mentioned that microwave techniques cannot be used to study plasmas with electron densities above about $10^{15}/cm^3$ due to the lack of readily available microwave sources at the present time.

While the microwave techniques have these two limitations, they do not require thermal equilibrium for the determination of free electron densities and thus may be used to advantage where the spectral line broadening and line intensity methods are inapplicable.

As has been pointed out previously, the most popular choice of a plasma model is the plane wave, "infinite slab" plasma; however, it has been shown that this model cannot be used indiscriminately (Refs. 70 and 71). Thus, one can make phase measurements with some degree of confidence in experimental arrangements where the theoretical hypotheses are not stringently satisfied, but amplitude measurements under the same conditions can lead to errors of several orders of magnitude in the deduced plasma properties.

In the most frequently used free-space propagation scheme, one measures the change in phase and attenuation due to the plasma of a propagating electromagnetic wave. In order to determine the change in phase, one must compare the wave transmitted through the plasma with the original wave and this leads to a bridge or interferometer arrangement.

We have found the arrangement depicted in Fig. 4 particularly useful in studies of the electrical properties of arc-heated argon and nitrogen plasma flows (Ref. 57). This apparatus, which operates in the 60-90 kmc range, employs a motor-driven phase shifter and is used to obtain only phase change information which leads directly to electron density. The amplitude measurements which yield collision frequencies are determined separately by a direct transmission experiment. The results obtained with these techniques agree quite well with results obtained using the cut-off criteria, i.e., $\omega = \omega_p$.

In the study of time-varying plasmas such as those produced by shock tubes, one must resort to faster methods of phase measurements such as those developed by Wharton (Ref. 12) and Osborne (Ref. 72). These methods have time resolutions of the order of 0·1 μsec, which is more than adequate for most measurements. An additional advantage with the interferometer method is that because it is a "null-balance" technique, it can be used in systems where the signal to noise ratio is quite low; a situation commonly encountered with turbulent plasma flows.

In the presence of a magnetic field, one usually seeks a method of measuring the rotation of the plane of polarization (Faraday rotation) under steady (Ref. 73) or transient conditions (Ref. 74).

For the diagnostics of steady-flow facilities, the rotation of the plane of polarization due to the plasma in the magnetic field may be obtained by rotating the plane of polarization of the incident electric field and plotting the transmitted signal incident upon an antenna which accepts only one plane of polarization. This can be accomplished using a rotating "half-wave" plate, unambiguous even for rotation angles greater than 360°. We have made measurements on arc-heated argon plasma flows using this technique (Ref. 57), but have found that one must be extremely careful in interpretation because of the severe magnetohydrodynamic effects that can occur.

If a portion of an electromagnetic wave incident upon a plasma is reflected,

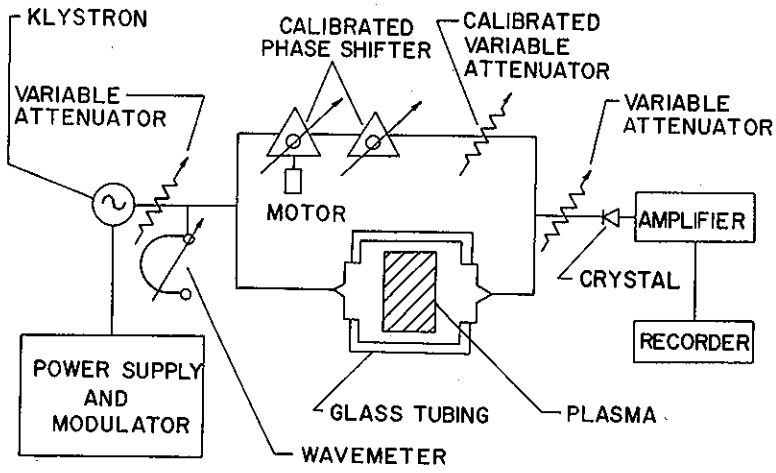

Fig. 4. Schematic of microwave interferometer.

transmission type experiments can yield misleading information concerning the plasma properties because the effect of reflections are manifested as an abnormally high attenuation coefficient. On the other hand, properly interpreted reflection measurements can yield significant information concerning plasma phenomena.

While transmission measurements are used to measure the properties of a plasma in a certain volume, reflection measurements tend to examine "surface" phenomena since they penetrate the plasma until the electron density is such that $\omega = \omega_p$ and total reflection occurs. This of course assumes that $\nu^2 \gg \omega^2$ because the effect of collisions is to smooth out any abrupt transitions in propagation phenomena.

If the plasma is contained in an apparatus such that the microwave signal must traverse the walls of the container, there will be a certain amount of reflected energy even in the absence of the plasma. Although these reflections

can be "tuned out" using matching techniques, they must be employed with considerable caution since the plasma reflected energy is not a simple additive contribution (Ref. 69).

OTHER PROPERTIES

A perusal of the diagnostic literature indicates that plasma diagnosticians have favored electrical conductivity measurements over the determination of the other transport properties. This is probably because a sufficiently high electrical conductivity is a necessary condition for the successful operation of many plasma devices. Also because of these the theory of electrical energy transport has been developed to considerable maturity. Unfortunately, there is relatively little information about the thermal conductivity of plasmas even though this must be known in designing reliable re-entry vehicles and direct-energy conversion devices. In our experiments described in detail by Knopp (Ref. 20) we use a modified wall-stabilized arc first proposed by Maecker. The plasma column is stabilized co-axially within a Vycor tube which is water cooled on the outside. The cooling of the tube gives rise to a thermal boundary layer within the tube and hence, the high-temperature plasma column is confined at the center of the tube. Thus, one obtains a cylindrically symmetrical plasma column. The gas to be studied is introduced co-axially into the tube and the steady flow has the effect of inhibiting radial convective energy transport from the axis to the wall. The flow is laminar and there are no eddy currents.

The equations governing the phenomena under consideration are the fluid mechanical conservation equations as well as the expressions for the conservation of charge and species. In determining the thermal conductivity it is the energy equation which is important and this is written as follows:

$$\sigma E^2 + \frac{1}{r}\frac{\partial}{\partial r}\left(r\kappa \frac{\partial T}{\partial r}\right) - q_{rad} = 0 \tag{53}$$

The quantities in this equation can be measured and from them the thermal conductivity $\kappa(T)$ can be determined. The electrical conductivity is calculated in accordance with Spitzer's theory. The crucial measurement is the accurate determination of the radial temperature distribution in the plasma column. This is done spectroscopically. It should be mentioned that in making the spectroscopic observations particular attention must be paid to the optical distortions created by the tube walls.

Viscosity and diffusivity

Our associate D. P. Aeschliman (Ref. 75) are presently exploring the feasibility of determining the plasma viscosity from the momentum equation. For an arc column one can write

$$\frac{\partial}{\partial r}\left(\mu \frac{\partial V_z}{\partial r}\right) + \frac{\mu}{r}\frac{\partial V_z}{\partial r} - \frac{\partial p}{\partial z} = 0 \tag{54}$$

The viscosity can be calculated from this equation directly because the pressure gradient can be measured with existing instrumentation. The velocity profile must be obtained from measurements of the velocity distribution. This last measurement does present complications but we are optimistic about using tracer particles.

The diffusivity may be calculated once reliable data for conductivity and viscosity are available.

Radiant energy transfer from plasmas

An appreciation of the radiative losses from plasmas is of particular interest in the design of large facilities such as magnetohydrodynamic power generators and hyperthermal arc windtunnel installations. Our colleagues, Berry and Tankin (Ref. 14) have used a thermistor bolometer to measure the radiation from argon and nitrogen plasmas. The radiation incident on the bolometer is chopped with a rotating disc at 30 cps and the resulting a.c. signal is fed to an amplifier. With this arrangement the total radiation, the actual radiative heat transfer, the distribution of the radiative flux along the plasma axis and the radiative power density of the plasma jet were determined. It was found that in the case of atmospheric argon plasma, the radiative loss may be as high as 18 per cent of the net power input to the plasma. In the case of nitrogen plasma the radiative energy transfer was found to be of the order of 1 per cent. Both bremmstrahlung and recombination radiation were found to be significant.

The authors extend their appreciation to many individuals and organizations which made possible the studies described in this paper.

We thank our colleagues in the Gas Dynamics Laboratory and particularly Professor Morris E. Brodwin who throughout our studies has given his wise counsel unstintingly and with a delightful sense of humor. We are grateful to Professors T. P. Anderson and R. S. Tankin who were generous with their advice throughout the preparation of this paper and on many other occasions.

Two of us (Richard C. Warder, Jr., and Ali Bulent Cambel) must thank our students for their diligent support. The preparation of this manuscript was made possible by the selfless cooperation of Mesdames Barbara Greer, Peggy Smykowski, and Joy Thornton who were instrumental in its typing.

The Research findings discussed in this paper were supported by the U.S. Air Force Office of Scientific Research under Contract No. AF OSR 49(638)-879 *and AF OSR Grant No.* 62-307*; The Arnold Engineering Development Center Contract No. AF AEDC* 40(600)-972, *The National Science Foundation under Grant No.* 917692, *Warnecke Electron Tubes, Inc., and Northwestern University.*

SYMBOLS

A_{nm} spontaneous transition probability
B_{nm} stimulated transition probability
$\vec{B}$ magnetic induction

B, C	experimentally determined constants
$\vec{E}$	electric field intensity
$E_{n,\ m}$	energy of nth and mth bound state
$\vec{H}$	magnetic field intensity
I	radiation intensity
$I(r)$	measured radial intensity distribution
I_{nm}	radiation intensity of bound transition between nth and mth excited states
$\vec{J}$	current density
K	dielectric coefficient
$N_{n,\ m}$	number of atoms (or ions) with electrons in the nth or mth excited state
$N_{e,\ i,\ a}$	particle number density of electrons, ions, or atoms, respectively
P	power input to arc
$Q_{i,\ a}$	internal partition function of the atom or ion
R_{nm}	rate per unit volume at which atoms (or ions) undergo bound state transitions from the excited n to the state m
T	translational temperature
T_e	electron temperature
T_g	gas or heavy particle temperature
$T_{i,\ a}$	ion temperature or atom temperature, respectively
$\vec{V}_e$	average drift velocity of electrons
V_z	plasma velocity component
X	ionization potential
Z	charge number
Z_{eff}	effective charge seen by the free electrons
C	speed of light
$C\rho$	specific heat at constant pressure
d	plasma width
g_i	statistical weight of the ground state of ion
$g_{n,\ m}$	statistical weight of the nth or mth bound state of atom or ion
h	Planck's Constant
k	Boltzmann's Constant
m	molecular weight
m_e	electron mass
m_H	heavy particle mass
$\vec{n}$	refractive index of the plasma
p	pressure
q_{rad}	radiative heat flux
$\vec{r}$	position vector
t	time
z	position
α	attenuation constant of the plasma
β	phase constant of the plasma
β_0	free space wave number or phase constant
γ	propagation constant

ε	plasma dielectric constant
ε_0	free space dielectric constant
ε_ν	continuum radiation per unit frequency
θ	angle of rotation
κ	thermal conductivity
λ_e	electron mean free path
λ	wave length
λ_0	wavelength of the unperturbed line
$\Delta\lambda_D$	Doppler half width of the broadened line
ν_{eff}	"effective" collision frequency
ν^e	mean rate of collisional excitation or de-excitation of the level in question by collisions of atoms (or ions) with electrons
ν_{nm}	characteristic frequency of radiation between bound states E_n and E_m
ξ	ellipticity
ρ	radiation energy density or mass density
σ	plasma conductivity
τ	relaxation time
$\Delta\Phi$	change in phase
ω	angular frequency of applied electromagnetic radiation
ω_c	cyclotron frequency
ω_p	electron plasma frequency
$\vec{\psi}$	electric or magnetic field
$\vec{\psi}_0$	amplitude of either the incident electric or magnetic field
μ	viscosity
μ_0	permeability of free space

REFERENCES

[1] "A Survey of Plasma Diagnostic Techniques" by the Vidya Staff; ARL Report 64–80, prepared under Contract AF 33(616)-8338, May 1964.

[2] Olsen, H. N., "Measurement of Argon Transition Probabilities Using the Thermal Arc Plasma as a Radiation Source," Speedway Laboratories Report, Linde Company, 1962.

[3] Knopp, C. F., "A Spectroscopic Technique for the Measurement of Temperature in Transparent Plasmas," M.S. thesis in Mechanical Engineering, Northwestern University, April 1961.

[4] Nighan, William L., "Microwave Diagnostics of an Arc-Heated Nitrogen Plasma," M.S. thesis in Mechanical Engineering, Gas Dynamics Laboratory, Northwestern University, August 1962.

[5] Thornton, J. A., "A Spectroscopic Study of the Argon Plasmas Generated in a Conical Type Electromagnetic Shock Tube," NU-GDL Report B-2-63.

[6] Smith, D. C., Briscoe, M. G., Anderson, T. P., and Cambel, A. B., "The Photography of Argon Plasmas," *Photographic Science and Engineering* **7**, No. 3, 177 (May-June 1963).

[7] Smith, D. C., Briscoe, M. G., and Cambel, A. B., "Photographic Study of Arc Initiation and Stabilization in a Plasma Jet," *ARS Journal* **32**, No. 7, 1097 (July 1962).

[8] Smith, D. C., "Investigation of the Feasibility of Colour Schlieren for Engineering

Applications," M.S. thesis in Mechanical Engineering, Gas Dynamics Laboratory, Northwestern University, September 1960.

[9] Klein, Alan F., "A Survey of Optical Interferometry as Applied to Plasma Diagnostics," *Physico-Chemical Diagnostics of Plasmas*, Ed. T. P. Anderson, R. W. Springer and Richard C. Warder, Jr., Northwestern University Press, Evanston, 1964, p. 233.

[10] Grey, J., Jacobs, P. F., and Sherman, M. P., "Calorimetric Probe for the Measurement of Extremely High Temperatures," *Rev. Sci. Instr.* **33**, 7 (1962).

[11] Fowler, R. G., "Electrically Energized Shock Tubes," Final Report to ONR Fluid Mechanics Branch, Project N9onr97700, 1963.

[12] Wharton, Charles B., "Plasma Diagnostic Techniques," *Physico-Chemical Diagnostics of Plasmas*, Ed. T. P. Anderson, R. W. Springer and Richard C. Warder, Jr., Northwestern University Press, Evanston, 1964, p. 3.

[13] Enright, J. A., "A Spectroscopic Determination of Temperature and Velocity Distributions in an Argon Plasma Jet," M.S. thesis in Mechanical Engineering, Gas Dynamics Laboratory, Northwestern University, June 1963.

[14] Berry, J. M., and Tankin, R. S. "An Experimental Study of Radiant Energy Transfer from a Plasma," NU-GDL Report No. A-1-64, 1963.

[15] Drellishak, K. S., Knopp, C. F., and Cambel, A. B., "Partition Functions and Thermodynamic Properties of Argon Plasma," *Phys. Fluids* **6**, No. 9, 1280 (September 1963).

[16] Drellishak, K. S., "Partition Functions and Thermodynamic Properties of High Temperature Gases," GDL Report prepared under AEDC Contract No. AF 40(600)–972, AEDC-TDR-64-22, January 1964.

[17] Drellishak, K. S., Aeschliman, D. P., and Cambel, A. B., "Tables of Thermodynamic Properties of Argon, Nitrogen and Oxygen," GDL Report prepared under AEDC Contract No. AF 40(600)–927, AEDC-TDR-64-12, January 1964.

[18] Bosnjakovic, F, and Springe, W., "Electrical and Thermal Conductivity of Argon Plasma," *Progress in International Research on Thermodynamic and Transport Properties*, Ed. J. F. Masi and D. H. Tsai, ASME, Academic Press, New York, 1962.

[19] Cann, A. L., "Energy Transfer Processes in a Partially Ionized Gas," GAL CIT Hypersonic Research Report prepared under Army Ordnance Contracts No. DA-04-495-Ord-1960 and 3231, June 15, 1961.

[20] Knopp, C. F., "An Experimental Determination of the Thermal and Electrical Conductivity of Argon Plasma," Ph.D. dissertation in Mechanical Engineering and Astronautical Sciences, Gas Dynamics Laboratory, Northwestern University, June 1964.

[21] Thornton, J. A. and Cambel, A. B., "A Spectroscopic Study of the Thermodynamic State of Argon Generated in a Conical Electromagnetic Shock Tube," *J. Quant. Spec. Radiat. Transfer.* **4**, 97 (1964).

[22] Spitzer, L., *Physics of Fully Ionized Gases*, Interscience, New York, 1956.

[23] Compton, K. T., "Mobilities of Electrons in Gases," *Phys. Rev.* **22** (November 1923).

[24] Compton, K. T., "On the Motions of Electrons in Gases," *Phys. Rev.* **22** (October 1923).

[25] Cambel, A. B., *Plasma Physics and Magneto Fluidmechanics*, McGraw-Hill, New York, 1963.

[26] Morse, T. F., "Energy and Momentum Exchange Between Nonequipartition Gases," *Phys. Fluids* **6**, 1420 (1963).

[27] Cambel, A. B., Duclos, D. P., and Anderson, T. P., *Real Gases*, Academic Press, New York, 1963.

[28] Duclos, D. P., "The Equation of State of an Ionized Gas," Ph.D. dissertation in Mechanical Engineering, Gas Dynamics Laboratory, Northwestern University, Evanston, August 1960; or AEDC-TN-60-192 prepared under Contract No. AF 40(600)–748, Arnold Engineering Development Center, October 1960.

[29] Rem, J. and Lewis, M. B., "An Investigation of the Thermodynamic Properties of a Plasma," GDL Tech. Note 61-1 ,March 1961, prepared under Contract No. AF 40(600)–748, Arnold Engineering Development Center.

[30] Bachynski, M. P., Shkarofsky, I. P., and Johnston, T. W., "Plasma Physics of Shock Fronts," Research Report No. 7-801-3, RCA Victor Ltd., Canada, June 1959, ASTIA-AD-245921.

[31] Fowler, R. G., "Radiation from Low Pressure Discharge," *Handbuch der Physik* **22**, Berlin, 1956, p. 209.

[32] ter Haar, D., *Elements of Statistical Mechanics*, Holt, Rinehart and Winston, New York 1960.

[33] Post, R., "Radiation Losses from Hot Plasma," *Plasma Dynamics*, F. H. Clauser, Addison-Wesley, Reading, Mass., 1960, p. 30.

[34] Kennedy, L. A., "Electrical Conductivity of Propane-Air Flames Seeded with Alkali Metal Compounds," M.S. thesis in Mechanical Engineering, Gas Dynamics Laboratory, Northwestern University, June 1962.

[35] Seemann, G. R., "Experimental Aspects of Magnetoaerodynamic Drag," NU-GDL Report C-1-63 prepared under Contract NSF G-17692, August, 1963.

[36] Penner, S. S., *Quantitative Molecular Spectroscopy and Gas Emissivities*, Addison-Wesley, Reading, Massachusetts, 1959.

[37] Gaydon, A. G. and Hurle, I. R., *The Shock Tube in High-Temperature Chemical Physics*, Reinhold, New York, 1963.

[38] Kerrebrock, J. L. and Hoffman, M. A., "Experiments on Nonequilibrium Ionization Due to Electron Heating," paper No. 64–27 presented at AIAA Aerospace Sciences Meeting, New York, January 20–22, 1964.

[39] Penner, S. S., "Optical Methods for Determining Flame Temperatures," *Am. J. Phys.* **17**, No. 7 (1949).

[40] Glennon, B. M. and Wiese, W. L., "Bibliography on Atomic Transition Probabilities," National Bureau of Standards Monograph 50, August 1, 1962.

[41] Wilson, R., "The Spectroscopy of Non-Thermal Plasmas," *J. Quant. Spec. Radiat. Transfer.* **2**, No. 4, 477 (Oct-Dec 1962).

[42] Griem, H. R., "Validity of Local Thermal Equilibrium in Plasma Spectroscopy," *Phys. Rev.* **131**, No. 3, 1170 (August 1963).

[43] Robben, F., "Electronic Rate Processes in Non-Equilibrium Plasmas," Preprint No. 64-56, American Institute of Aeronautics and Astronautics Meeting, New York, Jan. 20–22, 1964.

[44] Hinnov, E. and Hirschberg, J. G., "Electron-Ion Recombination in Dense Plasmas," *Phys. Rev.* **125**, No. 3, 795 (February 1, 1962.)

[45] Griem, H. R., "High-Density Corrections in Plasma Spectroscopy," *Phys. Rev.* **128**, No. 3, 997 (November 1, 1962).

[46] Pearce, W. J., "Plasma-Jet Temperature Measurement," *Optical Spectrometric Measurements of High Temperatures*, Ed. P. J. Dickerman, Univ. of Chicago Press, 1961, p. 125.

[47] Griem, H. R., "Plasma Spectroscopy," *Proceedings, Fifth International Conference on Ionization Phenomena in Gases*, Munich, 1961, North-Holland Publishing Company, Amsterdam, p. 1857.

[48] Rutgers, G. A. and DeVos, J. C., "Relation Between Brightness Temperature, True Temperature, and Color Temperature of Tungsten," *Physica* **20**, No. 10, 715 (October 1954).

[49] DeVos, J. C., "A Determination of the Emissivity of Tungsten Ribbon," *Physica* **20,** No. 10, 690 (October 1954).
[50] Nestor, O. H. and Olsen, H. N., "Numerical Method for Reducing Line and Surface Probe Data," *SIAM Review* **2,** No. 3, 200 (July 1960).
[51] Pomerantz, J., "The Influence of the Absorption of Radiation on Shock Tube Phenomena," *J. Quant. Spec. Radiat. Transfer.* **1,** 185 (1961).
[52] Unsöld, A., "Uber das kontinuierliche Spektrum der Hg-Hochdrucklamp, des Unterwasserfunkens und ähnlicher Gasentladungen," *Ann. Physik* **33,** No. 7, 607 (December 1938).
[53] Olsen, H. N., "Partition Function Cut-off and Lowering of the Ionization Potential in an Argon Plasma," *Phys. Rev.* **124,** 1703 (1961).
[54] Lochte-Holtgreven, W., "Production and Measurement of High Temperatures," *Report on Progress in Physics,* Vol. 21, The London Physical Society, 1958, p. 312.
[55] Griem, H., "Stark Broadening of Isolated Spectral Lines from Heavy Elements in a Plasma," *Phys. Rev.* **128,** p. 515 (1962).
[56] Warder, R. C., Jr., "Microwave Diagnostics of Arc-Heated Argon Plasma Flows," Ph.D. dissertation in Mechanical Engineering and Astronautical Sciences, Gas Dynamics Laboratory, Northwestern University, June 1963.
[57] Warder, R. C., Jr., Nighan, W. L., Brodwin, M. E., and Cambel, A. B., "Microwave Diagnostics of High Speed Plasma Flows," Proceedings of the VIth International Conference on Ionization Phenomena in Gases, Paris, France, 1964.
[58] Albini, F. A. and Jahn, R. G., "Reflection and Transmission of Electromagnetic Waves at Electron Density Gradients," *J. Appl. Phys.* **32,** 75 (January 1961).
[59] Wharton, C. B. and Slager, D. M., "Microwave Determination of Plasma Density Profiles," *J. Appl. Phys.* **31,** (February 1960).
[60] Warder, R. C., Jr. and Hector, D. L., "Microwave Determination of Anisotropic Plasma Electron Density Profiles," NU-GDL Report B-1-64, January 1964, submitted for publication.
[61] Carswell, A. I., "Microwave Scattering from Supersonic Plasma Flow-Fields," RCA Victor Research Report 7-801-24, January 1963.
[62] Carswell, A. I., Nuttall, J., and Paquette, G., "Electromagnetic Wave Scattering by Plasma Systems with Applications to the Re-entry Problem," RCA Victor Research Report No. 7-801-05, also DAMP Technical Monograph No. 62–24, December 1962.
[63] Shmoys, J., "Proposed Diagnostic Method for Cylindrical Plasmas," *J. Appl. Phys.* **32,** No. 4, 689 (April 1961).
[64] Tevelow, F. L. and Curchack, H. D., "Microwave Diagnostics in the Shock Tube," Diamond Ordnance Fuze Laboratories, TR-962, 1961.
[65] Lin, S. C., "Rate of Ionization behind Shock Waves in Air," *Electromagnetic Effects of Re-entry,* Pergamon Press, New York, 1961.
[66] Daiber, J. W. and Glick, H. S., "Plasma Studies in a Shock Tube," *Electromagnetics and Fluid Dynamics of Gaseous Plasma,* Polytechnic Press, New York, 1961.
[67] Jahn, R. G., "Microwave Probing of Ionized-Gas Flows," *Phys. Fluids* **5** (June 1962).
[68] Warder, R. C., Jr., Nighan, W. L., Brodwin, M. E., and Cambel, A. B., "Microwave Diagnostics of Arc-Heated Plasmas," *Dynamics of Manned Lifting Planetary Entry,* John Wiley, New York, 1963.
[69] Carswell, A. I., Bachynski, M. P., and Cloutier, G. G., "Microwave Measurements of Electromagnetic Properties of Plasma Flow Fields," *Physico-Chemical Diagnostics of Plasmas,* Ed. T. P. Anderson, R. W. Springer and R. C. Warder, Jr., Northwestern University Press, Evanston, 1964.

[70] Warder, R. C., Jr., Brodwin, M. E., and Cambel, A. B., "Sources of Error in the Microwave Diagnostics of Plasmas," *J. Appl. Phys.* **33** (September 1962).
[71] Bachynski, M. P., Cloutier, G. G., and Graf, K. A., "Microwave Measurements of Finite Plasmas," AFCRL-63-161, May 1963.
[72] Osborne, F. J. F., "A Multiple-Probe Microwave System for Plasma Studies," *Can. J. Phys.* **40**, 1620 (1962).
[73] Rao, K. V. N., Verdeyen, J. T., and Goldstein, L., "Interaction of Microwaves in Gaseous Plasmas Immersed in Magnetic Fields," AFCRL-62-489, April 1962.
[74] Consoli, T. and Dagi, M., "Measure de la Densité Electronique por Effect Faraday, *Vth International Conference on Ionization Phenomena in Gases*, Vol. 1, North-Holland Publishing Co., Amsterdam, 1962.
[75] Aeschliman, D. P., Ph.D. dissertation in progress, Mechanical Engineering and Astronautical Sciences, Gas Dynamics Laboratory, Northwestern University, June 1966.

DISCUSSION

RICHARD J. ROSA (Avco-Everett Research Laboratory, Everett, Massachusetts):

The paper of Thornton, Warder, and Cambel is an impressive compendium of information and literature on plasma generation and diagnosis, which I am sure will be most useful to workers in the field. As the authors themselves state, however, their work is largely oriented toward propulsive devices. Therefore I would like to add a few remarks based on the somewhat different experience at the Avco-Everett Research Laboratory in the areas of re-entry simulation and magnetohydrodynamic power generation. In these applications, the gas is typically dense, but slightly ionized, and seldom very far from thermodynamic equilibrium.

First, as regards batteries as a power supply for plasma jets—in the above-mentioned areas, there is usually a high premium on power but not much incentive to operate for more than a few seconds, or at the most, a minute. Moreover we seldom manage to make more than a few runs in any one day. Under these circumstances, battery banks have proven to be significantly more economical and flexible than other D.C. power supplies.[1]

Another source of plasma that should not be overlooked is the chemical combustion chamber, or rocket engine seeded with alkali metal salts. Again the virtue of this source to us has been its ability to supply plasma literally "by the ton" for detailed studies of the fluid mechanics of MHD generators.[2]

Still another plasma source which has proven useful in our generator work is a graphite pebble-bed type heater which can supply moderately high flows of seeded inert gas with closely controlled composition and temperature in the neighborhood of 2000°K.[3]

In these MHD generator experiments, we have more or less incidentally acquired an interesting tool for bulk plasma diagnosis.[3] We almost always find ourselves with a Hall effect that is relatively strong. Under these conditions, if we short-circuit the output of a Hall generator, for example, we obtain a quite accurate measure of electron density (average). Then a

comparison of this current with the current flow in the $\tilde{u} \times \tilde{B}$ direction gives a reasonably accurate measure of electron mean free time or mobility.

Finally, a measurement of conductivity by any of the several methods described by the authors gives the product of electron density and mean free time which serves as a check on the previous measurements. Thus we have a convenient, quite accurate, and foolproof way of measuring the bulk properties of most interest to us; and the deducing the electronic momentum transfer cross-sections of the various species in the energy range of a few tenths of an electron volt, a range not easily accessible by classical methods. Although only bulk, or average, properties are determined, we of necessity strive to make the flow in a generator as uniform as possible; and a measurement of open-circuit Hall voltage is a sensitive check of how well we have succeeded.[3]

REFERENCES

[1] Brogan, T. R., "Electric Arc Gas Heaters for Re-entry Simulation and Space Propulsion," Avco-Everett Research Laboratory Report 35, September, 1958, also ARS Paper 724-58.
Rose, P. H., Powers, W. E., and Hritzay, D., "The Large High Pressure Arc Plasma Generator: A Facility for Simulating Missile and Satellite Re-Entry," Avco-Everett Research Laboratory Report 56, May 1959, also ARS Report 838-59.
Rosa, R. J., "Physical Principles of Magnetohydrodynamic Power Generation," Avco-Everett Research Report 69, January 1960, also *Phys. Fluids* **4**, 182–194 (February 1961).

[2] Louis, J. F., Lothrop, J., and Brogan, T. R., "Fluid Dynamic Studies with a Magnetohydrodynamic Generator," Avco-Everett Research Laboratory Report 145, March 1963, also *Phys. Fluids* **7**, 110 (1964).

[3] Klepeis, James., and Rosa, R. J., "Experimental Studies of Strong Hall Effects and VXB Induced Ionization" Avco-Everett Research Laboratory Report 177, April 1964, also presented at the 5th Symp. on Engr. Aspects of Magnetohydrodynamics, MIT, Cambridge, Mass, April 1964.